NEURAL PROCESSING OF THE SAME, BEHAVIOURALLY RELEVANT FACE FEATURES IS DELAYED BY 40 MS IN HEALTHY AGEING

Katarzyna Jaworska[1±], Fei Yi[1], Robin A.A. Ince[1], Nicola J. van Rijsbergen[1], Philippe G. Schyns[1], and Guillaume A. Rousselet[1]

[1] Institute of Neuroscience and Psychology, University of Glasgow, Glasgow G12 8QB, United Kingdom

[±] Corresponding author: katarzyna.jaworska@glasgow.ac.uk

Abstract

Fast and accurate face perception is critical for successful human social interactions. Face perception declines with age both in behavioural and neural responses, although we do not yet understand why. Here, we tested the hypothesis that early brain mechanisms involved with face information processing are delayed in older participants. Using face detection - the most basic task for social interaction – we sampled visual information from faces (vs. noise) and reconstructed the features (mainly, the left eye) associated with detection behaviour in young (20-36 years) and older (60-86 years) adults. We then compared behavioural results to neural representations of face features revealed with simultaneously recorded EEG on the N170, an event-related potential associated with visual categorization. Whereas the right hemisphere N170 latency and amplitude represented the left eye in young participants, it was mostly amplitude that represented the eye with a 40 ms delay in older adults. Our results demonstrate that face processing speed declines in ageing with a delay in the early stages that process the visual information important for behaviour.

INTRODUCTION

Ageing impairs social tasks such as face perception, including face detection (Owsley, Sekuler, & Boldt, 1981; Norton, McBain, & Chen, 2009), face recognition (Boutet, Taler, & Collin, 2015), or emotion perception (Ruffman, Henry, Livingstone, & Philips, 2008). Such perceptual differences could impact everyday social interactions and decision-making in older adults. Behavioural differences in face categorization performance, such as configural processing (Slessor, Riby, & Finnerty, 2013; Chaby, Narme, & George, 2011), viewpoint invariance (Habak, Wilkinson, & Wilson, 2008), and efficiency of face information use (Rousselet, Husk, Pernet, Gaspar, Bennet, & Sekuler, 2009; Rousselet, Gaspar, Pernet, Husk, Bennet, & Sekuler, 2010) are suggestive of age-related decrements in neural processes associated with face perception, although deterioration of low-level perceptual capacities, such as acuity or contrast sensitivity, is also likely involved (Boutet et al., 2015).

Indeed, neuroimaging studies provide evidence for many age-related changes in the human visual system, which in turn could lead to slower processing (Rousselet et al., 2009, 2010), including reduced neuronal selectivity (Burianová, Lee, Grady, & Moscovitch, 2013; D. C. Park et al., 2004; J. Park et al., 2012), and lower functional variability of brain responses (Garrett, Kovacevic, McIntosh, & Grady, 2010). In particular, cross-sectional evidence suggests that face processing slows down by about 1 ms per year from 20 years of age onwards (Bieniek, Frei, & Rousselet, 2013; Rousselet et al., 2009, 2010). The onset of this age-related delay starts around 120 ms following stimulus onset, suggesting that the effect has a cortical origin (Bieniek, Bennett, Sekuler, & Rousselet, 2015; Bieniek et al., 2013). Consistent with this observation, the N170, an early event-related potential (ERP) component associated with face processing (Bentin, Allison, Puce, Perez, & McCarthy, 1996; Itier, Alain, Sedore, & McIntosh, 2007; Rousselet, Ince, van Rijsbergen, & Schyns, 2014; Schyns, Jentzsch, Johnson, Schweinberger, & Gosselin, 2003), is delayed in older participants (Gazzaley et al., 2008; Nakamura et al., 2001; Rousselet et al., 2009; Wiese, Schweinberger, & Hansen, 2008).

In addition to delayed visual processing, evoked responses in older adults might also reflect increased de-differentiated processing—e.g. increased processing of task-irrelevant information (e.g. non-diagnostic face features), or increased false alarms (e.g. noise textures processed as meaningful stimuli). Indeed, some studies have suggested an age-related increase in brain responses to non-preferred stimuli in visual areas that respond

preferentially to one stimulus category in young adults (Park et al., 2012). Similar de-differentiation of EEG responses could occur in occipital-temporal brain regions. Specifically, Rousselet et al. (2009) reported a prominent peak in the time window of the N170 in response to noise textures in older participants (see also Bieniek et al., 2015; Rousselet et al., 2010), suggesting that the N170 might become less face-sensitive with age (Rousselet et al., 2009).

Despite the breadth of age-related differences in behavioural and neural responses, there is no direct link between the two that enables an understanding of the functional significance of the brain responses supporting behaviour in face perception tasks in older adults. In young adults, we have previously shown that pixels in the contra-lateral eye region primarily modulate N170 responses, suggesting that one function of the N170 is to code the presence of an eye (Rousselet et al., 2009; Schyns, Petro, & Smith, 2007; Smith, Gosselin, & Schyns, 2004; Van Rijsbergen & Schyns, 2009; Ince, Jaworska, Gross, Panzeri, van Rijsbergen, Rousselet, & Schyns, 2016). However, age-related studied of the N170 have been based on categorical responses to whole faces. Thus, although we know that older adults have delayed ERP responses to faces (Rousselet et al., 2009), it remains unclear how this delay maps onto face processing specifically.

Here, we addressed this broad question by quantifying information processing in the most basic face-processing task, face detection, in young and older participants. To this aim, we used the Bubbles technique (Gosselin & Schyns, 2001) that randomly samples information from the stimulus on each trial. We coupled the Bubble information sampling method with reverse correlation and information theoretic measures, to first reveal what facial information is associated with behavioural responses and then to reveal where and when this task-relevant information is processed in the dynamic response of the brain measured with single-trial EEG.

RESULTS

PRESENCE OF THE LEFT EYE MODULATED REACTION TIMES IN BOTH GROUPS

Young (median age = 23) and older (median age = 66) participants categorized 2,200 pictures of faces and noise textures revealed through Gaussian apertures ("Bubbles", Gosselin & Schyns, 2001) that sample random spatial regions of face and noise images on each trial.

Young participants detected faces faster than older participants (median RT young = 378 ms, 95% confidence interval = [349, 401] vs. older 576 ms [527, 604]; group difference = 198 ms [148, 237]). To understand the face information associated with these RTs, we computed Mutual Information (MI; see *Materials and Methods*), which quantifies non-parametrically the relationship across trials between the visibility of each individual pixel and RT.

Presence of the left eye modulated RTs of all young participants, and almost all older participants (N young = 17/17 vs. N older = 16/18; Figure 1A-B, top panel; see also Rousselet et al., 2014). Presence of the right eye also modulated RTs in a few young and older participants.

PRESENCE OF THE EYES WAS CRUCIAL FOR OLDER PARTICIPANTS TO DETECT A FACE

Young participants detected faces more accurately than older participants (bubble trials, mean young = 93% [92, 94] vs. older = 82% [80, 85]; group difference = 11 percentage points (PP) [8, 14]), although both groups reached 98% [97, 98] on practice trials in which face and noise images were presented without bubbles. Older adults found the Bubbles task more challenging (bubble-practice difference, young = -4 PP [-6, -3] vs. older = -15 PP [-18, -11]; group difference = -11 PP [-14, -7]). Specifically, older participants had higher numbers of noise responses on face trials, while both groups were similarly accurate on noise trials (face trials, young = 91% correct vs. older = 75% correct; group difference = 15 PP [8, 19]; noise trials, young = 95% vs. older = 92%; group difference = 4 PP [1, 13]; group difference of face-noise difference = 7 PP [0, 15]).

To understand the face information associated with behaviour, we used MI to compute the relationship between pixel visibility and correct vs. incorrect responses. Eye region pixels were strongly associated with correct responses in only a few young participants and almost

all older participants, suggesting that young participants used any feature to do the task, in contrast to older participants who needed to see the eye region to correctly detect a face (N young = 4/17, N older = 16/18, Figure 1A-B, third panel). This reliance on the eyes was confirmed in the average classification image of the difference between the groups (see Figure 1C, third panel).

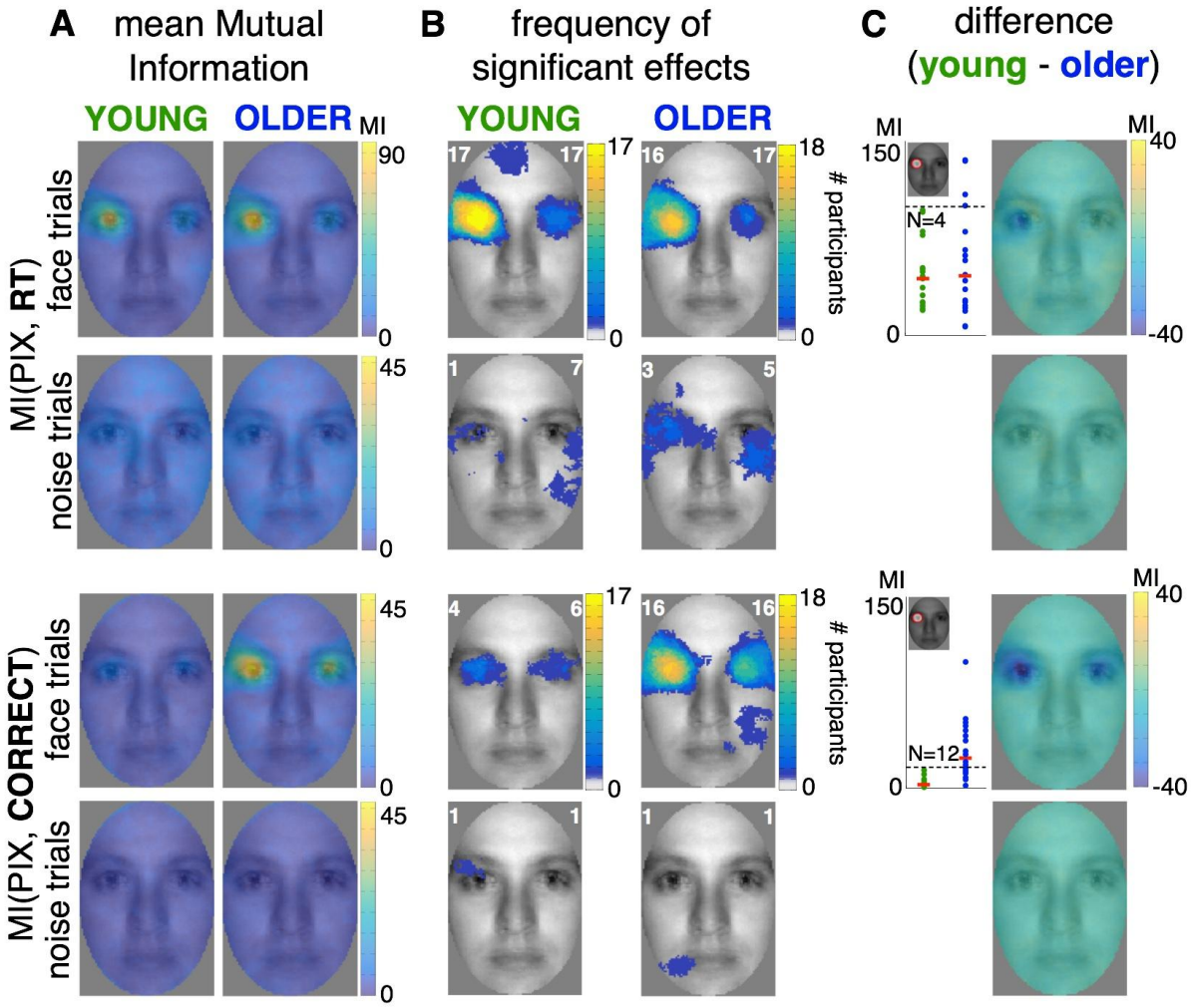

Figure 1 Age-related differences in behavioural classification images.

(A) Group-average MI maps (units: scaled MI, see *Materials and Methods*). The maximum average MI on face trials was stronger for reaction times (RT) than for accuracies (CORRECT) for both age groups and is therefore presented on a different scale. **(B) Frequency of significant effects**. The white number in the left upper corner of every image corresponds to the maximum number of participants showing a significant effect at the same pixel, whereas the number in the right upper corner corresponds to the total number of participants showing significant effects at any pixel. **(C) Differences in MI between young and older participants**. Scatterplots show individual MI values averaged within the left eye mask (represented as a red circle in the face inset; for explanation, see

Methods). Red bars correspond to medians across participants. Distributions of individual MI values were different between the groups, with 12 older participants showing stronger MI than the maximum across young participants for MI(PIX, CORRECT); and 4 older participants for MI(PIX, RT). Images on the right display the differences between young and older average MI maps for each response measure and stimulus category.

We confirmed these results with a reverse analysis (see *Materials and Methods*) that showed, in young adults, a 53 ms RT gain [45, 61] and 15 percentage points (PP) accuracy gain [10, 20] when the left eye was visible – vs. 91 ms [68, 114] and 37 PP [25, 48] gains in older participants (Figure 2). For the right eye, these gains were respectively 17 ms [10, 24] and 7 PP [4, 11] in young participants; and 16 ms [2, 30] and 28 PP [19, 36] in older participants (see Table S3 in Supplementary Material for effect sizes of group differences).

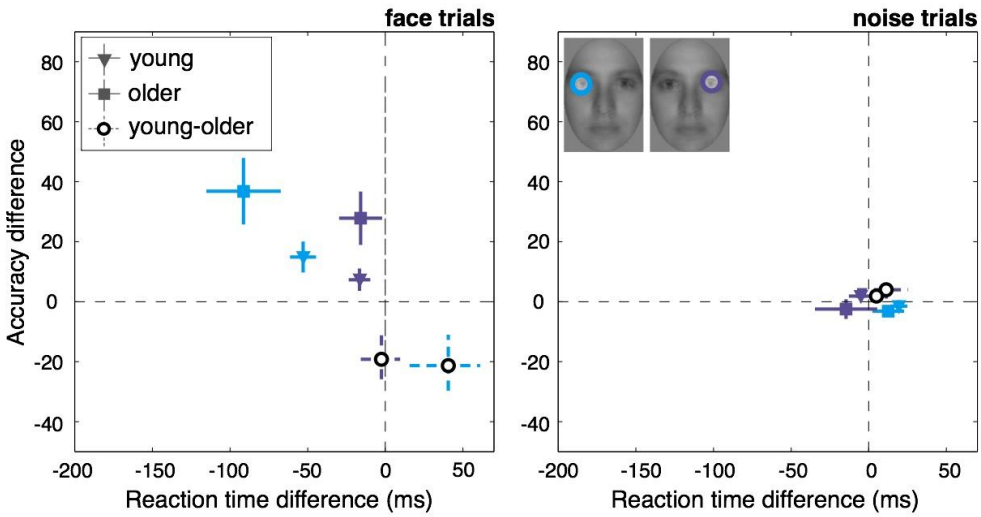

Figure 2 Behavioural modulation by eye visibility. Each point corresponds to the median difference between high and low visibility of the left (blue) and the right (purple) eye, separately for young (triangles) and older (squares) participants, and for face (left panel) and noise (right panel) trials. Vertical and horizontal lines mark 95% confidence intervals (CI) for accuracy and reaction time differences, respectively. Group differences (empty circles and dashed CI lines) show stronger modulation of accuracy scores by the presence of each eye in older participants, as well as stronger RT modulation by the presence of the left eye.

To demonstrate a difference in behavioural strategy between the groups, Figure 3 (bottom panel) shows that on trials without any eye visibility (either left or right), young participants could still detect faces accurately, whereas older participants could not (bin 1, young: min = 56%, median = 72%, max = 92%; older: min = 9%, median = 31%, max = 94%; see also Supplementary Figures S2 – S4 for reaction times, and for noise trials).

In sum, our behavioural RT and accuracy results reveal that all participants used the left eye to detect faces from noise. However, whereas the eyes were all older participants could use to make correct responses, young participants could also use any other face feature; demonstrating a strategy difference in older participants.

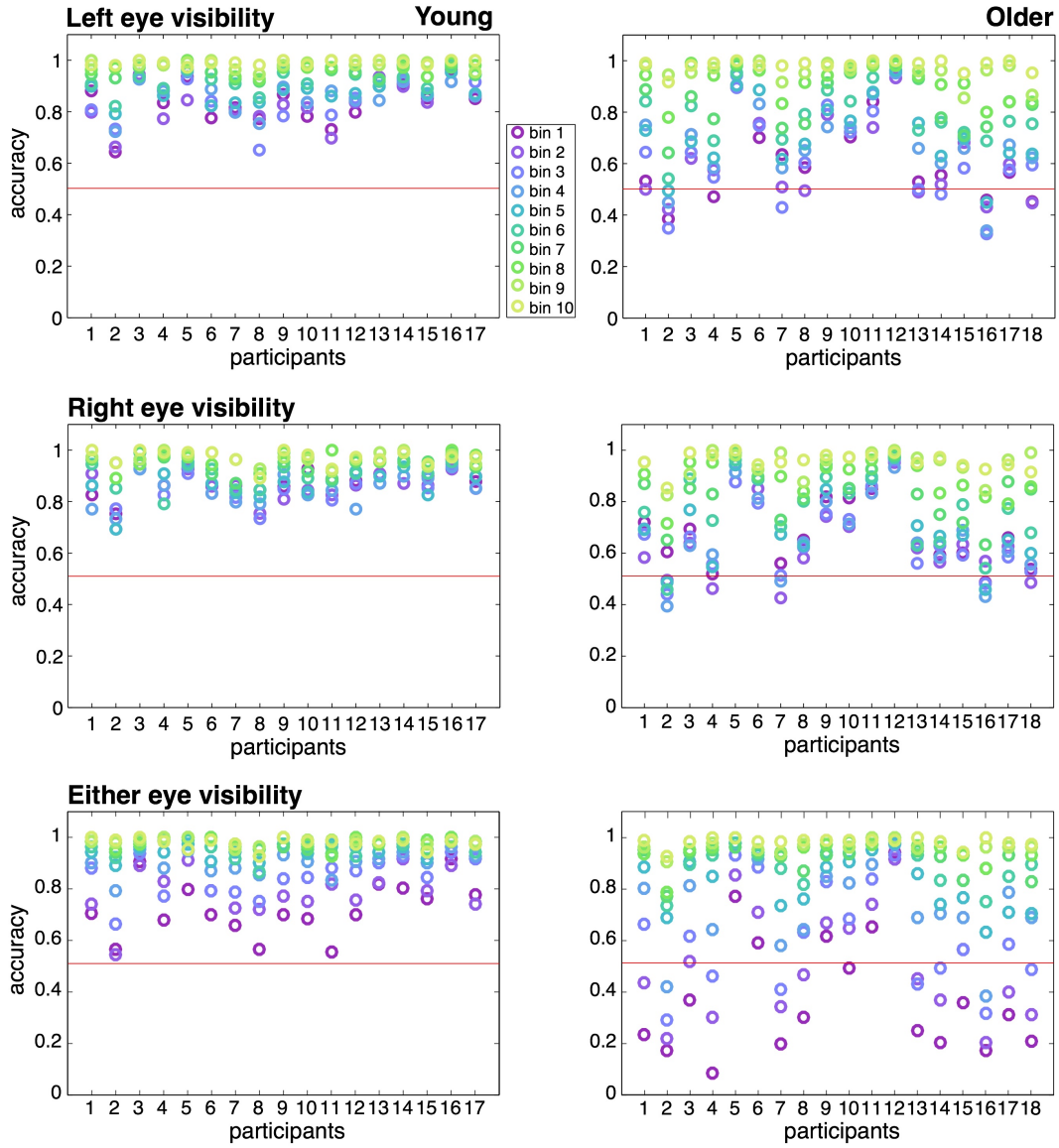

Figure 3 Reverse analysis, face trials. Each column of dots presents one participant's accuracy scores averaged within each of the 10 bins of visibility of the left eye (top), the right eye (middle), or either eye (bottom) from bin 1 (low visibility), to bin 10 (high visibility). Young (left) and older (right) participants' scores are presented separately. Low eye visibility (low bin numbers and purple to blue colours) was associated with lower accuracies. This association was particularly visible across older participants when there was no eye visibility in either eye region (bottom right panel). Red horizontal lines represent chance level.

AGEING EFFECTS ON THE MEAN N170 COMPONENT

As expected, the N170 of young and older participants differed in latency on face and noise trials, and between trials with and without (practice) Bubbles: the N170 peaks were delayed in older participants by 18 ms [9, 24] in practice face trials, and by 23 ms [9, 38] in practice noise trials; by 22 ms [10, 32] in Bubble face trials, and by 18 ms [7, 31] in Bubble noise trials (Figure 4; for effect size estimates of group differences, see Table S4 in Supplementary Material). The N170 amplitude differed only on practice noise trials, with older participants having much larger responses to noise than young participants.

More interestingly, we can analyse how single-trial ERPs varied in response to the stimulus information revealed through the Gaussian apertures. To this end, using MI we computed the information content of face trials, as well as noise trials.

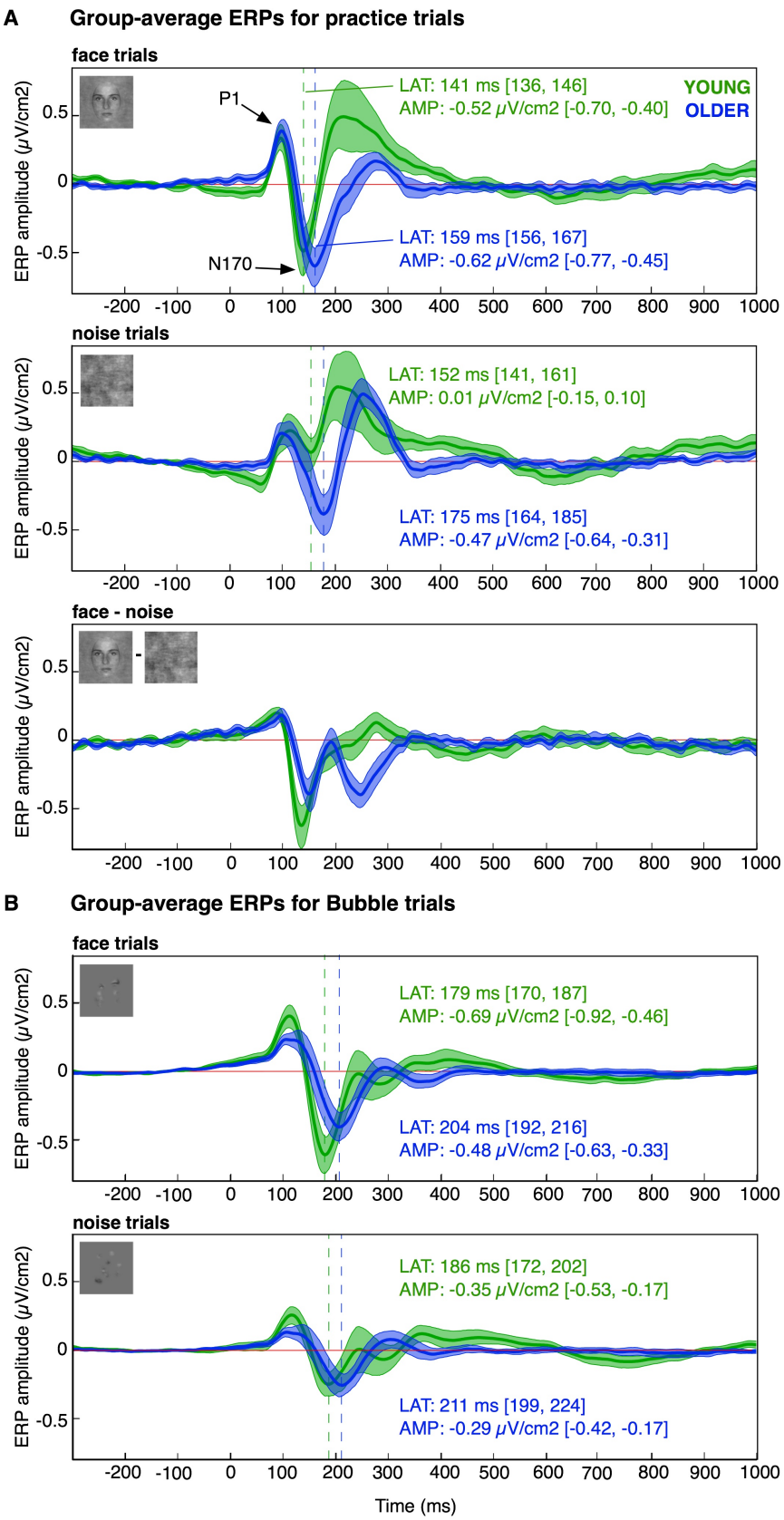
A
Group-average ERPs for practice trials
face trials
P1
N170
LAT: 141 ms [136, 146]
AMP: -0.52 μV/cm2 [-0.70, -0.40]
YOUNG
OLDER
LAT: 159 ms [156, 167]
AMP: -0.62 μV/cm2 [-0.77, -0.45]
noise trials
LAT: 152 ms [141, 161]
AMP: 0.01 μV/cm2 [-0.15, 0.10]
LAT: 175 ms [164, 185]
AMP: -0.47 μV/cm2 [-0.64, -0.31]
face - noise
B
Group-average ERPs for Bubble trials
face trials
LAT: 179 ms [170, 187]
AMP: -0.69 μV/cm2 [-0.92, -0.46]
LAT: 204 ms [192, 216]
AMP: -0.48 μV/cm2 [-0.63, -0.33]
noise trials
LAT: 186 ms [172, 202]
AMP: -0.35 μV/cm2 [-0.53, -0.17]
LAT: 211 ms [199, 224]
AMP: -0.29 μV/cm2 [-0.42, -0.17]
ERP amplitude (μV/cm2)
0.5
0
-0.5
-200 -100 0 100 200 300 400 500 600 700 800 900 1000
Time (ms)

1

Figure 4 Group-average ERPs. **(A) Practice trials.** Thick lines correspond to ERPs averaged across young (green) and older (blue) participants, for face and noise trials separately, and for the difference between face and noise trials (third panel). Shaded areas correspond to 95% confidence intervals. Values reported in the panels correspond to median latencies and amplitudes of the N170 component. **(B) Bubble trials.**

PRESENCE OF THE EYES MODULATED BRAIN ACTIVITY IN BOTH GROUPS

We used MI to reveal the features that modulated single-trial EEG responses on the left and right lateral-occipital electrodes (i.e. LE and RE) and midline occipital electrode (Oz) between 0 and 400 ms post-stimulus. As shown in Figure 5, presence of the eye contralateral to the recording electrode modulated EEG responses (see Figures 5A and 5B), with a stronger response to the left eye recorded at RE in both groups.

Eye sensitivity exceeded a family-wise error rate permutation threshold in a smaller number of older than young participants and was overall weaker in older participants (see Figures 5B and 5C). To quantify this effect, we averaged MI within a circular eye mask in each participant separately (see Figure 5 caption) and computed Cliff's *delta* measure of effect size: the effect size was large both at LE and RE (Cliff's *delta*, LE = 0.58 [0.21, 0.81]; RE = 0.57 [0.19, 0.80]). The midline electrode (Oz, Figure 5A, bottom panels) revealed weaker associations and sensitivity to various face features (eyes, chin, mouth, nose, and forehead) in some participants in both age groups on face trials.

To rule out a mere effect of spatial attention (rather than eyes per se), we computed MI on noise trials and found no systematic sensitivity to the eyes in either group (Figure 5), although there was some sensitivity to the left cheek area in a few older participants.

We also ensured not to miss any effects by computing the same classification images across all electrodes; they showed sensitivity to the left eye region in both groups (see Figure S4 in Supplementary Material).

In sum, these results extend former results of contralateral eye coding in face detection in young participants (Rousselet et al., 2014; Ince et al., 2016), and add the weaker association for older adults, which contrasts with their stronger reliance on the eyes for behavioural RT and accuracy.

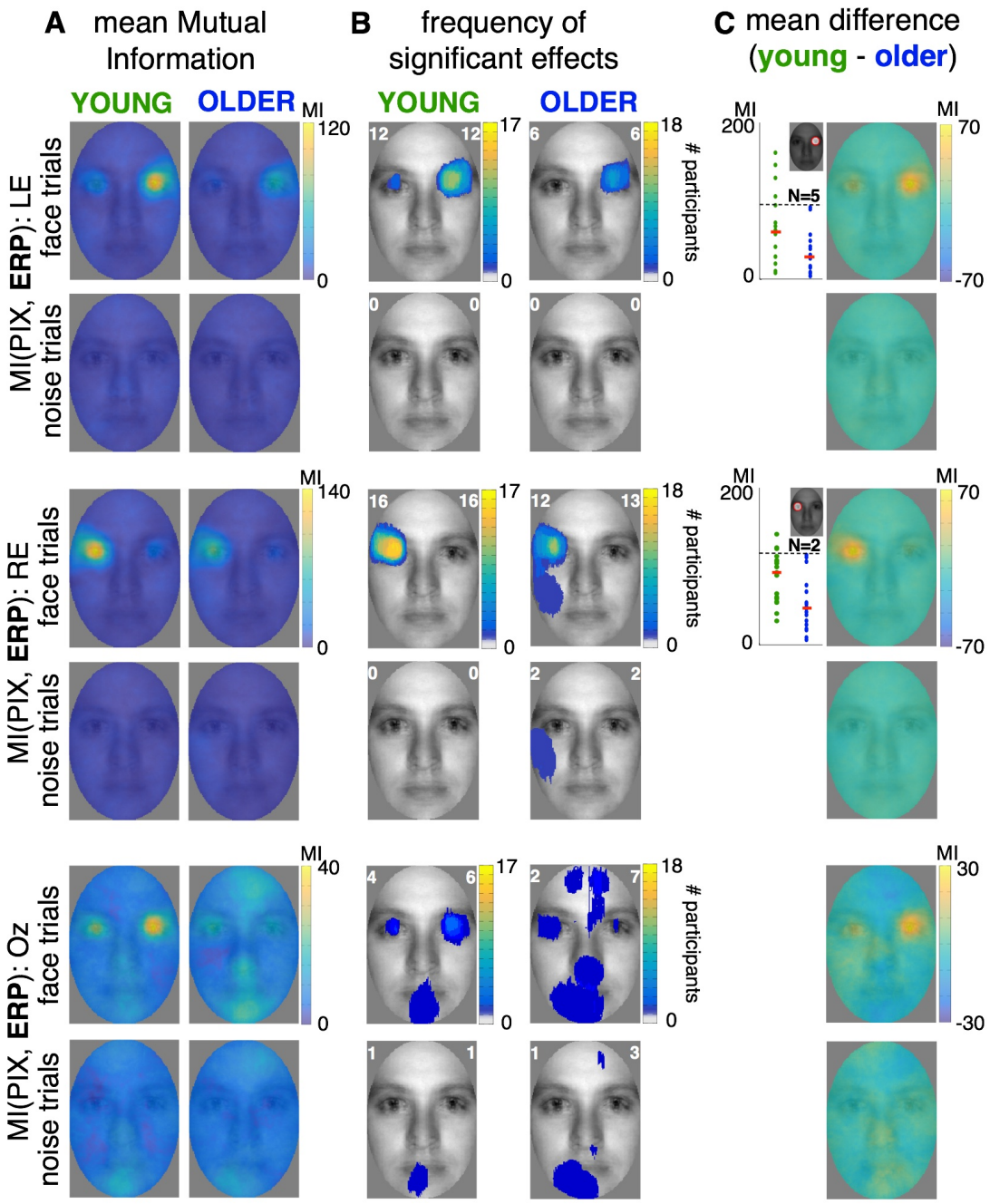

Figure 5 Age-related differences in ERP information content.

(A) Mean Mutual Information. Group-average MI maps for young (left) and older (right) participants, displayed for the left (LE) and right (RE) lateral occipital-temporal electrodes, and the midline occipital electrode (Oz) independently for face and noise trials. The classification images for face and noise trials show maximum MI values across time points. RE showed significant MI to the left cheek area in 2 older participants in noise trials, suggesting some sensitivity to low-level image features that was absent in young participants. **(B) Frequency of significant effects**. The white number in the left

upper corner of every image corresponds to the maximum number of participants showing a significant effect at the same pixel, whereas the number in the right upper corner corresponds to the total number of participants showing significant effects at any pixel. **(C) Differences in mean MI between young and older participants**. The scatterplot to the left of the image shows individual MI values averaged within the right eye mask (for the left electrode), or the left eye mask (for the right electrode). The number in each scatterplot corresponds to the number of young participants whose MI values were greater than the maximum MI value across older participants (marked as a black dashed line). The image on the right displays the difference between average young and older MI maps for every condition.

EYE SENSITIVITY IS DELAYED AND WEAKER IN OLDER ADULTS

Knowing what face information was associated with ERP responses, we then investigated how this relationship unfolded over time. To this aim, we plotted the maximum MI across pixels in each classification image between 0 and 400 ms post stimulus (see Figure 6B), and computed the MI peak latencies for young and older participants.

MI peaked around 165 ms in young participants and around 205 ms in older participants at both LE and RE (Figure 6B). Thus, we observed a 40 ms delay in coding of the eye information in older, compared with young, participants (95% CI for the median difference in ms, LE = [28, 65]; RE = [23, 57]).

We also confirmed weaker eye sensitivity in older adults across time: the peak MI amplitude in older participants was about 58% of that of young participants at LE and 57% at RE (95% CI, LE = [36, 89]; RE = [42, 82]).

At the midline electrode, we observed only weak and inconsistent group differences either in MI peak latencies, or peak amplitudes (MI peak latency, young = 162 ms [154, 180]; older = 154 ms [148, 172]; group difference = 3 ms [-13, 19]); see also Figure 6B, bottom panel).

Altogether, these results confirm the weaker eye sensitivity in older adults at electrodes covering the occipital-temporal regions, suggesting different representations of task-relevant features in the two age groups. Weaker coding of task-relevant face features was also delayed by about 40 ms in older participants.

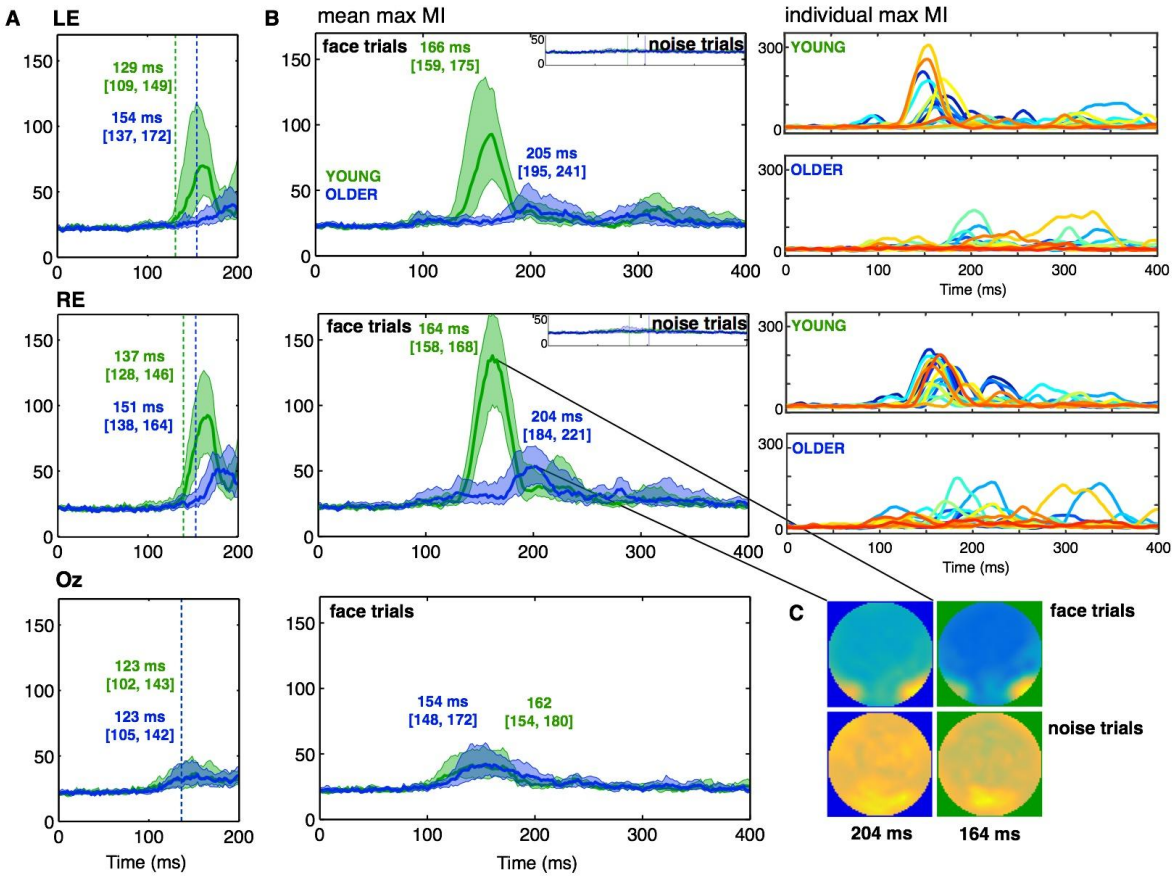

Figure 6 Time-courses of the maximum MI across pixels.

(A) Causal-filtered data. Time-courses of average MI values are presented for young (green) and older (blue) participants, for face trials only. The vertical lines mark the onset of the group effect. **(B) Non-causal-filtered data.** Time-courses of average MI values are presented for both face and noise (insets) trials. Colour-coded numbers correspond to median latencies of maximum MI in both groups, obtained for face trials. The two panels on the right display individual participants' time-courses. In all graphs, shaded areas correspond to 95% confidence intervals around the 20% trimmed mean. **(C) Group-averaged topographic maps.** Whole-scalp MI was strongest at posterior-lateral electrodes, and tended to be right lateralised in both groups (lateralisation index for face trials, young = -0.18 [-0.31, -0.05]; older = -0.23 [-0.37, -0.09]; group difference = 0.07 [-0.07, 0.21]).

ONSETS OF AGE-RELATED DELAYS IN INFORMATION PROCESSING

Having quantified an age-related difference in the timing of maximum eye-sensitivity, we wanted to determine if this timing difference was also present in the earliest measurable EEG eye sensitivity, and if this difference could be explained by a non-specific delay in visual activity. To answer these questions, we used causal-filtered data, to more precisely identify the timing of early effects (see Figure 6A; see also *Materials and Methods*).

First, we measured the onsets of MI to the eye features. The results suggest that the earliest eye sensitivity is already delayed in older participants. Median onsets of MI to the eye features in young participants were: 129 ms [109, 149] at LE, and 137 ms [128, 146] at RE. In older participants, MI onsets occurred slightly later: at 154 ms [137, 172] at LE, and at 151 ms [138, 164] at RE (group differences: 25 ms [5, 46] at LE, 13 ms [1, 24] at RE).

Second, we estimated onsets of cortical activity, to test whether the MI onset group differences could be explained by a general delay in the onset of visual cortical activity in older participants. To this aim, we looked at the time course of the standard deviation across electrodes of the mean ERP (ERP_{STD}, see *Materials and Methods*). Onsets of ERP_{STD} correspond to the initial activation in the occipital cortex after stimulus presentation (Foxe and Simpson, 2002), and could shed light on whether any age-related delay might already be present in the early stages of the visual processing pathway. Here, the onsets occurred at 68 ms [64, 72] in young participants, and at 69 ms [62, 75] in older participants (Figure 7). Importantly, we found very weak differences in the onsets of ERP_{STD} across the two groups (difference = -0.5 ms [-7, 5]), suggesting no general delay in the onset of visual cortical activity in older participants.

As such, our results suggest that the observed delay in the processing of the eye region is not due to a general age-related delay in the initial activation of the occipital-temporal cortex. Instead, the eye processing delay seems to occur later in the visual cortical processing pathway, thus ruling out low-level optical factors as the main contributor to the delay.

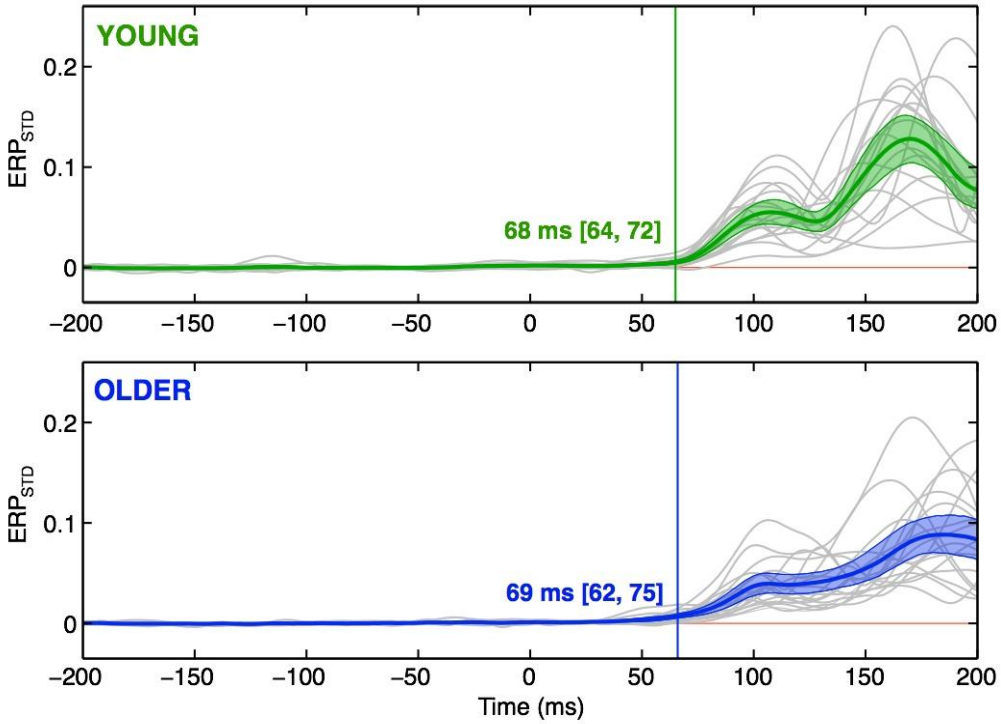

Figure 7 Onsets of afferent activity to the visual cortex.

Thin grey lines show individual participants' ERP_{STD} (μV/cm^2), the thick line shows the group average, and the shaded areas show 95% confidence intervals around the group mean. The vertical lines mark the onset of cortical activity in each group.

N170 LATENCY AND AMPLITUDE CODE THE PRESENCE OF THE EYES DIFFERENTIALLY IN YOUNG AND OLDER ADULTS

So far, we have shown stronger reliance on the eyes for behavioural performance in older participants in a face detection task, in contrast to their weaker and delayed eye coding over the occipital-temporal EEG electrodes. This weaker and delayed coding occurred in the time window of the N170, an ERP component associated with face categorization, and was not associated with any general delay in afferent activity to the visual cortex. Specifically, MI peaked about 10 ms earlier than the N170 in young participants, a relationship that was weaker or reversed in older participants (young, LE = 10 ms [4, 24]; RE = 8 ms [0, 16]; older, LE = 0 ms [-31, 8]; RE = 5 ms [-4, 18]; see also Rousselet et al., 2014).

To uncover the functional role of the N170 in coding task-relevant information in older adults, using a reverse analysis we sought to directly investigate how eye processing related to the N170 latency and amplitude (Figure 8; see *Materials and Methods;* see also Smith et al., 2004; Rousselet et al., 2014). As shown below (see Figure 8), we found that pixels in the contralateral eye region modulate amplitude and latency distributions of single-trial N170 in young participants (Rousselet et al., 2014), but mostly amplitude distributions in older participants.

Specifically, the N170 reconstructed from trials with high contralateral eye visibility on RE preceded and was larger than the N170 reconstructed from trials with low contralateral eye visibility (latency effect, young = 24 ms [17, 31] vs. older = 5 ms [-2, 11]; for amplitude effects, see Table 5). This latency effect was weaker at LE (young = 12 ms [8, 17]; older = 1 ms [-6, 9]), stronger in young than in older participants (for effect size estimates, see Table 4), and stronger at RE than LE in young compared to older participants (young = -7 ms [-12, -3] vs. older = -3 ms [-7, 3]; group difference = -5 ms [-15, 0]). Surprisingly, contralateral eye amplitude modulation at LE was *weaker* in young than in older participants, while similar across groups at RE (LE, young = 153% [140, 166]; older = 191% [157, 225]; see also Tables 4 and 5).

The presence of the ipsilateral eye had opposite effects on the N170 latency in the two groups: high ipsilateral eye visibility was associated with earlier N170 in young participants and later N170 in older participants (RE, young = 2 ms [1, 4] vs. older = -4 ms [-1, -8]; LE, young = 6 ms [2, 10] vs. older = -4 ms [-1, -8]).

In sum, our results suggest that ageing affects the N170 coding of the eye by showing that contra-lateral eye pixels modulate the amplitude and latency of the N170 in young participants (Rousselet et al., 2014), and mostly amplitude in older participants.

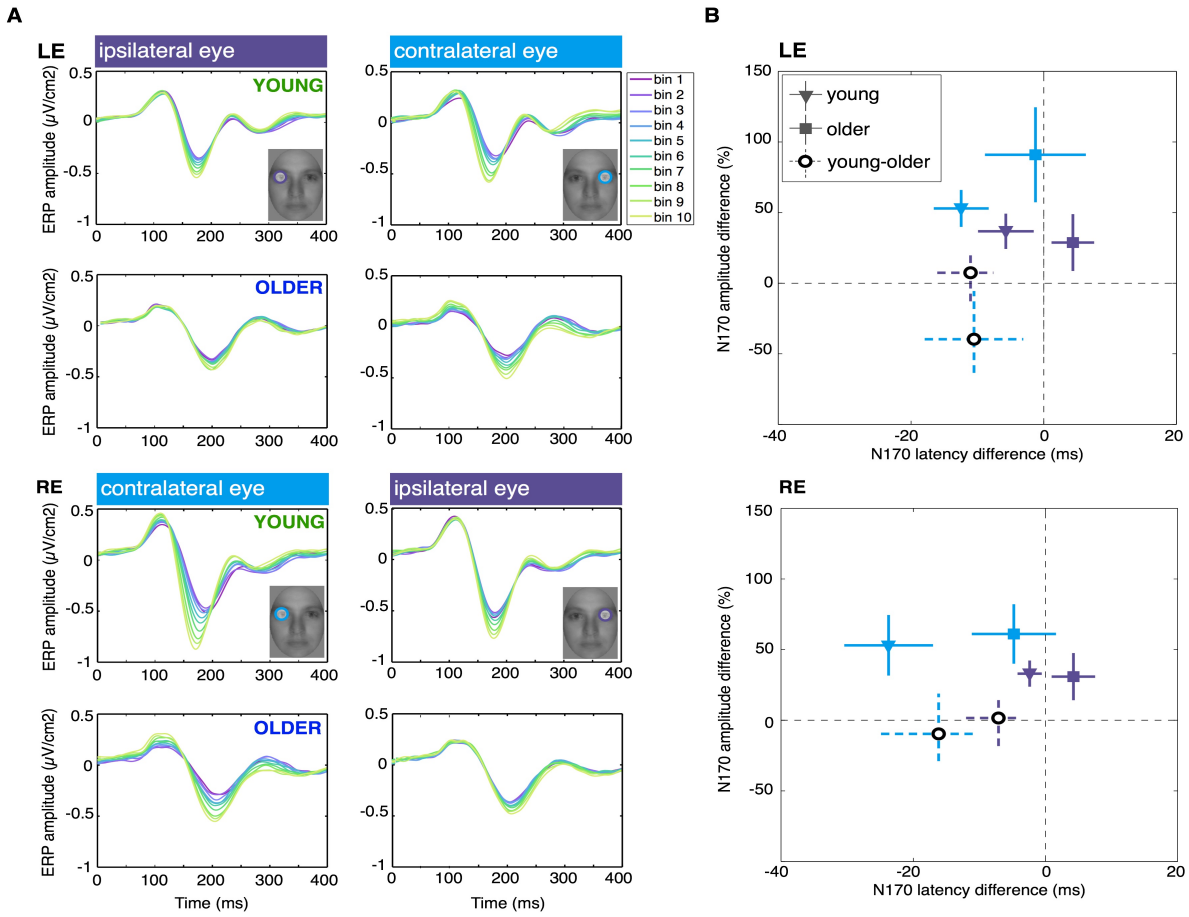

Figure 8 ERP modulation as a function of eye visibility in face trials.

(A) Binned ERPs. Rows correspond to face trials in young and older participants at the left electrode (top two), and at the right electrode (bottom two). Columns correspond to ERP modulations as a function of the visibility of the contralateral eye (blue) or the ipsilateral eye (purple). In young, but not in older participants, presence of the contralateral eye was associated with earlier and larger N170, particularly at the right electrode. **(B) Quantification of eye visibility effects on the N170 latency and amplitude**. Presented are effects of eye visibility (differences between the 10th, high information, and the 1st, low information, bin) on the N170 latency and amplitude, at the left (top) and right (bottom) lateral electrodes. Amplitude and latency modulations by the presence of the contralateral eye (blue) and ipsilateral eye (purple) are presented in both plots. Amplitude differences are expressed as proportion of the 1st bin ERP amplitudes: an amplitude difference of 50% means that amplitude of bin 10 ERPs was 150% the size of the amplitude of bin 1 ERPs. Filled circles correspond to median ERP modulations across young participants; squares show medians across older participants; empty circles show differences between group medians. Vertical and horizontal bars correspond to 95% confidence intervals.

Table 4 Effect size estimates for N170 eye coding.

Effect size estimates for group differences (young-older) in N170 latency (LAT) and amplitude (AMP) for different facial features visibility, at left (LE) and right electrodes (RE). Values correspond to differences in median latencies in milliseconds, and median amplitudes in percentage points. Square brackets indicate 95% confidence intervals. A corresponding Cliff's delta estimate is shown in italics.

	N170 LAT		N170 AMP	
	LE	RE	LE	RE
Left eye	-11 [-16, -7] *-0.79* *[-0.97, -0.56]*	-16 [-24, -11] *-0.77* *[-0.92, -0.52]*	7 [-14, 22] *0.16* *[-0.24, 0.58]*	-10 [-31, 17] *-0.16* *[-0.54, 0.20]*
Right eye	-11 [-18, -3] *-0.48* *[-0.80, -0.11]*	-7 [-12, -4] *-0.71* *[-0.92, -0.44]*	-40 [-64, -3] *-0.41* *[-0.76, -0.02]*	2 [-17, 14] *0.03* *[-0.39, 0.41]*

Table 5 N170 amplitude modulation by eye visibility.

N170 amplitude modulation for left and right eye visibility, at left (LE) and right (RE) electrode. Amplitude differences are expressed as proportion of the 1st bin ERP amplitudes, i.e. amplitude modulation of 137% means that amplitude of the 10th bin ERPs was 137% the size of the amplitude of the 1st bin ERPs. Square brackets indicate 95% confidence intervals.

	Young		Older	
	LE	RE	LE	RE
Left eye	137% [125, 150]	153% [132, 175]	129% [111, 150]	161% [141, 181]
Right eye	153% [140, 166]	133% [124, 142]	191% [157, 225]	131% [113, 149]

DISCUSSION

To understand visual information processing in ageing, we must start by asking what information the aged brain processes and when. Here, for the first time in a sample of older participants, we address these two questions by using reverse correlation to link facial stimulus space to behavioural and brain responses.

In terms of behaviour, older adults used pixels in the eye region to detect faces, similarly to young adults. In particular, pixels in the left eye region were associated with faster reaction times in both young and older participants, although the association was stronger in older than in young participants. Both groups were also more accurate when the left eye was visible. However, whereas young participants performed well above chance even when there was no eye visibility on a given trial, older adults struggled to respond correctly on those trials and performed below chance, with a bias towards reporting face absence. As such, young adults were able to do the task based on any feature revealed through Bubble masks, whereas older adults were heavily dependent on the presence of the eyes to detect faces. Altogether, our results align with previous literature showing decrements in older adults' performance in face perception tasks (Owsley, Sekuler, & Boldt, 1981; Norton et al., 2009; Slessor et al., 2013; Rousselet et al., 2009, 2010; Habak et al., 2008; Chaby et al., 2011; Obermeyer et al., 2012), and extend it by showing *what* specific information is necessary for older participants to correctly detect a face. Our results suggest that older participants used a different strategy to perform face detection – they seemed to be more conservative in only responding 'face' when the eyes were visible on a given trial. This strategy difference was unlikely due to shifts in spatial attention to the eye regions. If that were the case, we should observe Mutual Information (MI) due to spatial location of Bubbles in the eye region on noise and face trials alike. However, we only observed weak MI in a few participants, and no modulation of behavioural responses by presence or absence of Bubbles in the eye region on noise trials, yielding insufficient evidence for the spatial attention shift hypothesis. Instead, older adults might have to rely more on local contrast information contained within the eye region of the face, in line with previous studies showing that they require more contrast to detect and discriminate faces (Lott, Haegerstrom-Portnoy, Schneck, & Brabyn, 2005; Owsley, Sekuler, & Boldt, 1981). Increased reliance on higher contrast information might arise from blurred vision due to, for example, presbyopia (Koretz, Kaufman, Neider, & Goeckner, 1989). Although we tested each participant's contrast sensitivity and visual acuity,

unfortunately at present we cannot rule out a level of blur for the older group, given that participants wore their habitual visual correction – which might have been insufficient to allow clear vision at the viewing distance in our study. However, the fact that we observed larger N170 to noise textures in older than in young participants suggests that blur is an unlikely factor, as it should affect all responses irrespectively of their category. In addition, blur should affect all response latencies. However, cortical onsets were very similar between groups, providing another argument against the effect of blurred vision on observed behavioural or neural responses.

Having established what information participants use to perform a face detection task, we quantified when and where that information modulated brain activity. In young and older participants alike, we found that single-trial ERPs are mostly associated with the presence of eye pixels contralateral to the lateral-occipital recording electrodes. This association (measured with MI) was also stronger at right hemisphere electrodes in both groups, in line with the right hemisphere dominance for face processing (Sergent, Ohta, & MacDonald, 1992). However, MI was, on average, weaker in older participants. MI time courses also peaked about 40 ms later in older than in young participants suggesting that sensitivity to the same face feature is weaker and delayed in ageing. Importantly, there was no general delay in the onset of visual cortical activity in older participants, suggesting that the delay observed at lateral-occipital electrodes occurred at cortical information-processing stages and was unlikely to be due to retinal factors (Bieniek et al., 2013, 2015).

The eye sensitivity peaked about 10 ms before the peak of the N170 in young participants, and at the same time as the N170 in older adults (with the N170 itself being delayed in ageing; Gazzaley et al., 2008; Nakamura et al., 2001; Rousselet et al., 2009; Wiese, Schweinberger, & Hansen, 2008). We further quantified coding of the eye by the N170 using reverse analysis (Rousselet et al., 2014; Smith et al., 2004). Higher eye visibility was associated with larger amplitude of the N170 in young and older participants alike. However, there was only a weak modulation of latency in older participants, contrary to young participants. The N170 modulation by the contralateral eye was also larger in the right hemisphere in young, but not in older participants, in line with previous results showing reduced hemispheric asymmetry in older participants (Cabeza, 2002; De Sanctis et al., 2008). Altogether, our results suggest that the same diagnostic information (the contralateral eye) is processed in the same time window of the N170 in young and older participants, implying that the functional role of the N170 remains the same across the two groups.

However, this processing is associated with a different temporal pattern, where information peaks at the same time as the N170 in older participants and is only associated with a very weak change in latency.

Our behavioural and EEG results suggest a double-dissociation in age-related differences in face processing: a stronger reliance on the eyes in making behavioural judgments is coupled with weaker and delayed brain sensitivity to these features in older adults, relative to young adults. A similar dissociation was reported in an fMRI study investigating face perception from images degraded with noise in young and older adults (Grady, Randy McIntosh, Horwitz, & Rapoport, 2000). The highest correlation between brain activity and behavioural performance in a face matching task was found in the fusiform gyrus in young participants, but in posterior occipital regions in the older adults (Grady et al., 2000). In addition, two other areas – thalamus and hippocampus – showed positive associations with behaviour in a sample of older participants only, suggesting functional plasticity in the recruitment of brain areas responsible for face processing in old age. In line with these findings, a more recent study reported increased correlation between accuracy scores and greater recruitment of the face-processing network comprised of the fusiform gyrus and the orbitofrontal gyrus in older adults (Burianova et al., 2013). The compensatory recruitment of frontal regions in older adults specifically was hypothesized as a mechanism to counteract altered domain-specific processing in more posterior regions (Davis, Dennis, Daselaar, Fleck, & Cabeza, 2008), a hypothesis debated in light of more recent evidence (Morcom, CamCAN, & Henson, 2017).

Given the fMRI findings that suggest recruitment of different brain regions in face perception processes in ageing (Burianova et al., 2013; Park et al., 2004; Grady et al., 2000), it is important to note that our MI results were not biased by the selection of electrodes. Specifically, if other brain areas contributed to processing of faces in older adults in the current study, then restricting the analyses to occipital-temporal sensors in the left and the right hemisphere could lead to missing or poorly quantifying effects. We ensured we did not miss any local effects by running the MI analysis on all electrodes and visualising maximum MI across electrodes. Whole-scalp results, however, were very similar to those obtained at the electrodes of interest analysis, suggesting that occipital-lateral electrodes showed maximum sensitivity to the eye region in both young and older participants. Furthermore, results from a multivariate MI analysis between eye sampling and top PCA components showed that considering whole-scalp distribution of EEG activity in the two groups did not alter the difference in maximum MI or age-related delay. Altogether, analyses restricted to a

single lateral-occipital electrode in each hemisphere were sufficient to describe age-related differences in processing of facial information in our study.

The age-related delay in processing of the eye could not be attributed to the presence of Bubble masks either. Bubbles can be thought of as a form of masking procedure that degrades the visual input and has been suggested to entail object completion (Tang et al., 2014). Processing occluded stimuli by the visual system may require additional resources to perform the task, leading to longer processing times (Sekuler, Gold, Murray, & Bennett, 2000). As such, any delay observed in a sample of older adults could be due to a combination of factors: a genuine slowing down of processing speed, as well as an increase in the time needed to process the occluded stimulus with respect to young adults. However, our ERP results show that the processing time of Bubbled images compared with full images was not different in young and in older participants. Specifically, even though processing of the Bubbled stimuli was delayed with respect to full images by about 20 ms in both young and older participants, there was no interaction between age and masking condition. In both practice (unmasked) and Bubble (masked) trials, the N170 latency to face images in older participants was delayed by about 20 ms (18 ms in practice trials and 22 ms in Bubble trials) with respect to that in young participants. This is in line with a recent study (Bieniek et al., 2013) showing that even though stimulus luminance affects the entire ERP time course in both young and older participants, it does not affect age-related differences in processing speed.

On the other hand, there is behavioural evidence for an age-related difference in the perception of partially occluded objects. For example, older participants were less accurate and needed more stimulus information in tasks requiring perceptual closure (Cremer & Zeef, 1987; Salthouse & Prill, 1988; Whitfield & Elias, 1992), perceptual organization (Kurylo, 2006), contour integration (Roudaia, Bennett, & Sekuler, 2008) or perception of incomplete/fragmented figures (Danziger & Salthouse, 1978; Lindfield & Wingfield, 1999; Lindfield, Wingfield, & Bowles, 1994). In line with those findings, in our study both young and older adults were less accurate on Bubble trials compared with practice trials, but the drop in performance was much more pronounced across older participants.

The reason for such age-related deterioration in performance on tasks involving perception of fragmented pictures or perceptual closure remains elusive. It has been suggested that perceptual difficulties arise as a consequence of heightened noise or variability associated

with internal stimulus representation in the neural system (Salthouse & Lichty, 1985), or as a result of a deficit in inhibitory control of interfering/irrelevant information (Lindfield et al., 1994). In our study, ERP variance across Bubble trials, measured at the time point of max MI was slightly lower in older than in young participants (see Supplementary Figure S6), in line with recent fMRI studies showing that older adults modulate BOLD activity less than young adults (for a review, see Grady & Garrett, 2014), and indicating a reduction in variability-based neural specificity (Garrett et al., 2013; Takahashi et al., 2009). Interestingly, dividing each participant's max MI by their corresponding variance diminished group differences in coding strength, suggesting that stimulus coding was achieved in both groups using the full dynamic range of neural responses available to the participants, even though older adults had a lower dynamic range of responses overall (Garrett, Lindenberger, Hoge, & Gauthier, 2017). Furthermore, we also observed prominent early sensory responses in older adults to meaningless stimuli – textures – in line with previous studies showing increased general responses to visual stimuli without functional significance (Bieniek et al., 2015; De Sanctis et al., 2008; Kolev, Falkenstein, & Yordanova, 2006; Rousselet et al., 2009), and suggesting low differentiation of both within-, and between-stimulus responses. Importantly, we only observed very weak MI on noise trials in a few participants, suggesting that elevated mean ERP responses in older adults were unlikely to be driven by sensory processing of textures as meaningful stimuli. Another possibility is that the lower dynamic range of neural responses might be due to lower contrast from stimulus (itself due to optical factors such as blur, presbyopia). As stimulus contrast is important for driving neural responses in the visual cortex, the consequence of a blurred input may result in weaker and slower neuronal responses in the visual cortex, in turn leading to degraded perceptual abilities (Polat et al., 2012). However, for the reasons described above, blur is an unlikely explanation of the lower dynamic range of responses.

To summarize, our results provide the first functional account that advancing age involves differences in the earlier stages of processing visual information important for behaviour. Specifically, we show for the first time that the information content of early visual ERPs in older adults does not differ from that of young adults. While the contralateral eye region modulates ERPs in young and older adults alike, information processing is weaker and delayed in ageing. Furthermore, ageing affects coding of the eye by the N170 differentially: whereas eye visibility is associated with an amplitude change in older adults, it is associated with both a latency and amplitude change in young adults. These ERP findings are coupled

with an increased reliance on the presence of the eyes to produce behavioural responses in older adults, suggesting a change in strategy with age.

Materials and Methods

Participants

Eighteen young (9 females, median age = 23, min 20, max 36) and nineteen older adults (7 females, median age = 66, min 60, max 86) participated in the study. Results from fifteen of the young participants have been reported previously (Rousselet et al. 2014). All older adults were local residents, recruited through advertising at the University of Glasgow, active age gym classes, and a newspaper article. Volunteers were excluded from participation if they reported any current eye condition (i.e., lazy eye, glaucoma, macular degeneration, cataract), had a history of mental illness, were currently taking psychotropic medications or used to take them, suffered from any neurological condition, had diabetes, or had suffered a stroke or a serious head injury. Volunteers were also excluded from participation if they had their eyes tested more than a year (for older volunteers) or two years (for young volunteers) prior to the study taking place. Two older participants reported having cataracts removed, and one older participant reported having undergone a laser surgery. These participants were included because their corrected vision was within normal limits. Participants' visual acuity and contrast sensitivity were assessed in the lab during the first session using a Colenbrander mixed contrast card set and a Pelli-Robson chart. All participants had normal or near-normal visual acuity as measured with the 63 cm viewing distance (computer distance) chart (Table 1). Three older participants had contrast sensitivity of 1.65, and all others had contrast sensitivity of 1.95 log units. Both values fell within the normal range of contrast sensitivity for that age group (Elliott, Sanderson, & Conkey, 1990). All young participants had contrast sensitivity of 1.95 log units or above. During the experimental session, participants wore their habitual correction if needed.

Table 1. Visual test scores.

Visual acuity scores are reported for high contrast (HC) and low contrast (LC) charts presented at the 63 cm viewing distance, and expressed as raw visual acuity scores (VAS). The corresponding logMAR scores are presented below in italics. Square brackets indicate the minimum and maximum scores across participants in each age group. Contrast sensitivity (CS) scores for young and older participants correspond to median log units across all participants in each age group.

	HC 63	**LC 63**	**CS**
young	108 [95, 110]	99 [94, 104]	1.95 [1.95, 2.25]
	-0.16 [0.10, -0.20]	*0.02 [0.12, -0.08]*	
older	98 [93, 105]	89 [82, 95]	1.95 [1.65, 1.95]
	0.04 [0.14, -0.10]	*0.22 [0.36, 0.10]*	

The study was approved by the local ethics committee at the College of Science and Engineering, University of Glasgow (approval no. FIMS00740), and conducted in line with the British Psychological Society ethics guidelines. Informed written consent was obtained from each participant before the study. Participants were compensated £6/h.

STIMULI

We used a set of 10 grey-scaled front view photographs of faces, oval cropped to remove external features, and pasted on a uniform grey background (Gold, Bennett, & Sekuler, 1999). The pictures were about 9.3° x 9.3° of visual angle; the face oval was about 4.9° x 7.0° of visual angle. A unique image was presented on each trial by introducing phase noise (70% phase coherence) into the face images (Rousselet, Pernet, Bennett, & Sekuler, 2008). Textures were created by randomising the phase of the face images (0% phase coherence). All stimuli had the same amplitude spectrum, set to the mean amplitude of the face images. Face and texture images were revealed through 'bubble masks', i.e. masks containing 10 two-dimensional Gaussian apertures (sigma = 0.36°), with the constraint that the center of the aperture remained in the face oval (Rousselet et al., 2014). Information sampling was sufficient for the reported performance level (Rousselet et al., 2014). We wrote our experiments in MATLAB using the Psychophysics Toolbox extensions (Brainard, 1997; Kleiner, Brainard, & Pelli, 2007; Pelli, 1997).

PROCEDURE

Participants came in for two experimental sessions on separate days. During each session, we asked participants to minimise movement and blinking, or blink only when hitting a response button. The viewing distance of 80 cm was maintained with a chinrest.

In each experimental session, participants completed 12 blocks of 100 trials each while seated in a sound-attenuated booth. The first block was a practice block of images without bubble masks. A set of 10 face identities and 10 unique noise textures, each repeated 5 times were randomized within each block. Each session lasted about 60 to 75 minutes, including breaks, but excluding EEG electrode application.

Within a block of trials, participants were asked to categorise images of faces and textures as fast and accurately as possible by pressing '1' for face, and '2' for texture on the numerical pad of a keyboard, using the index and middle finger of their dominant hand. After each block, participants could take a break, and they received feedback on their performance in the previous block and on their overall performance in the experiment (median reaction time and percentage of correct responses). The next block started after participants pressed a key indicating they were ready to move on.

Each trial began with a small black fixation cross (12 x 12 pixels, 0.4° x 0.4° of visual angle) displayed at the centre of the monitor screen for a random time interval of 500 to 1000 ms, followed by an image of a face or a texture presented for 7 frames (~82 ms). After the stimulus, a blank grey screen was displayed until the participant responded. The fixation cross, the stimulus and the blank response screen were all displayed on a uniform grey background with mean luminance of ~43 cd/m^2.

EEG RECORDING AND PRE-PROCESSING

EEG data were recorded at 512 Hz using a 128-channel Biosemi Active Two EEG system (Biosemi, Amsterdam, the Netherlands). Four additional UltraFlat Active Biosemi electrodes were placed below and at the outer canthi of both eyes. Electrode offsets were kept between ±20 μV.

EEG data were pre-processed using MATLAB 2013b and the open-source EEGLAB toolbox (Delorme et al., 2011; Delorme & Makeig, 2004). Data were first average-referenced and detrended. Two types of filtering were then performed. First, data were band-pass filtered

between 1 Hz and 30 Hz using a non-causal fourth order Butterworth filter. Independently, another dataset was created in which data were pre-processed with fourth order Butterworth filters: high-pass causal filter at 2 Hz and low-pass non-causal filter at 30 Hz, to preserve accurate timing of onsets (Acunzo, MacKenzie, & van Rossum, 2012; Luck, 2005; Rousselet, 2012; Widmann & Schröger, 2012).

Data from both datasets were then downsampled to 500 Hz, and epoched between -300 and 1000 ms around stimulus onset. Mean baseline was removed from the causal-filtered data, and channel mean was removed from each channel in the non-causal-filtered data in order to increase reliability of Independent Component Analysis (ICA) (Groppe, Makeig, & Kutas, 2009). Noisy electrodes and trials were then detected by visual inspection of the non-causal dataset, and rejected on a subject-by-subject basis. Following visual inspection, one young participant and one older participant were excluded from further analyses due to noisy EEG signal. Mutual Information (MI) analysis confirmed the lack of sensitivity to any facial features in these participants. The resulting sample size was 17 young and 18 older participants. In this sample, more noisy channels were on average removed from older than from young participants' datasets (older participants: median = 10, min = 0, max = 24; young participants: median = 5, min = 0, max = 28; median difference = 4 [2, 7]). More noisy Bubble trials were also removed from older than from young participants' datasets (trials included in analyses, older participants: median 2130, min 1987, max 2180; young participants: median 2178, min 2023, max 2198; median difference = 42 [23, 64]).

Subsequently, ICA was performed on the non-causal filtered dataset using the Infomax algorithm as implemented in the *runica* function in EEGLAB (Delorme & Makeig, 2004; Delorme, Sejnowski, & Makeig, 2007). The ICA weights were then applied to the causal filtered dataset to ensure removal of the same components, and artifactual components were rejected from both datasets (median = 4, min = 1, max = 27 for one older participant who displayed excessive blink activity; the second max was 17). Then, baseline correction was performed again, and data epochs were removed based on an absolute threshold value larger than 100 μV and the presence of a linear trend with an absolute slope larger than 75 μV per epoch and R^2 larger than 0.3. The median number of bubble trials accepted for analysis was, out of 1100, for older participants: face trials = 1069 [min=999, max=1092]; noise trials = 1067 [min=986, max=1088]; for young participants: face trials = 1090 [min=1006, max=1100]; noise trials = 1089 [min=1014, max=1098]. Finally, we computed single-trial spherical spline current source density waveforms using the CSD toolbox (J.

Kayser, 2009; Tenke & Kayser, 2012). CSD waveforms were computed using parameters 50 iterations, m=4, lambda=10^{-5}. The head radius was arbitrarily set to 10 cm, so that the ERP units are μV/cm^2. The CSD transformation is a spatial high-pass filtering of the data, which sharpens ERP topographies and reduces the influence of volume-conducted activity. CSD waveforms also are reference-free.

ELECTRODE SELECTION

Detailed analyses were performed on a subset of electrodes. The set of electrodes consisted of four posterior midline electrodes that have been previously shown to be sensitive to face features or conjunction of features: from top to bottom CPz, Pz, POz, Oz (Rousselet et al., 2014; Schyns, Thut, & Gross, 2011). However, we report the results only from the Oz electrode because the other three showed weak mutual information values across the two groups. We also selected two posterior-lateral electrodes, one in the right hemisphere (right electrode, RE), and one in the left hemisphere (left electrode, LE). These electrodes were selected by measuring the difference between all bubble face trials and all bubble noise trials at all posterior-lateral electrodes, squaring it, and selecting the left and the right electrodes that showed the maximum difference in the period 130-250 ms. The selected lateral electrodes were P7/8, or PO7/8, or their immediate neighbours, which are electrodes typically associated with large face ERPs in the literature.

EVENT-RELATED POTENTIALS

We compared the amplitude and latency of the N170 between the two age groups. To this end, we computed mean ERPs across trials for each participant, separately for face and noise trials, and for practice (without Bubbles) and regular (with Bubbles) trials. For ERPs recorded at the lateral-occipital electrode in the right hemisphere (RE), we defined the N170 peak in individual participants as the minimum mean ERP between 110-230 ms, and considered separately its latency and amplitude.

STATISTICAL ANALYSES

Statistical analyses were conducted using Matlab 2013b and the LIMO EEG toolbox (Cyril R Pernet et al., 2011). Throughout the paper, square brackets indicate 95% confidence intervals computed using the percentile bootstrap technique, with 1000 bootstrap samples. Unless otherwise stated, median values are Harrell-Davis estimates of the 2nd quartile (Harrell & Davis, 1982).

Measures of effect size

We estimated the size of the between-group differences using two robust techniques: Cliff's delta and the median of all pairwise differences. Cliff's *delta* (Cliff, 1996; Wilcox, 2006) is related to the Wilcoxon-Mann-Whitney *U* statistic and estimates the probability that a randomly selected observation from one group is larger than a randomly selected observation from another group, minus the reverse probability. Cliff's *delta* ranges from 1 when all values from one group are higher than the values from the other group, to -1 when the reverse is true. Completely overlapping distributions have a Cliff's *delta* of 0. In line with Cliff's delta approach, we also calculated all pairwise differences between young and older participants on the measures of interest (reaction times, percent corrects, N170 latencies and amplitudes), and took the median of the distribution of these differences. This way of measuring effect sizes enabled us to provide information about the typical difference between any two observations from two groups (Wilcox, 2012).

Mutual Information

We used mutual information (MI) to quantify the dependence between stimulus features and behavioural and brain responses. MI is a non-parametric measure that quantifies (in bits) the reduction in uncertainty about one variable after observation of another and has been used to study the selectivity of neural and behavioural responses to external stimuli (Ince et al., 2017; Ince, Petersen, Swan, & Panzeri, 2009; S. J. Kayser, Ince, Gross, & Kayser, 2015; H. Park, Ince, Schyns, Thut, & Gross, 2015; Schyns et al., 2011). The advantage of using the MI lies in its ability to detect associations of any order, whether linear or non-linear (for a more extensive evaluation, see Rousselet et al., 2014). We calculated MI from the standard definition (Cover & Thomas, 2006), using the following formula:

$$I(B_i; R) = \sum_{b,r} P(b,r) log_2 \frac{P(b,r)}{P(b)P(r)}$$

We binned pixel visibility, as well as behavioural and electrophysiological responses into three equiprobable bins (Rousselet et al., 2014). As such, B_i represents the bubble mask value (pixel visibility) at pixel *i* and *R* represents the response of interest (either behavioural or EEG recording). *P(b)* is the probability of pixel *i* having bubble mask falling inside bin *b*; *P(r)* is the probability of the considered response falling inside bin *r*, and *P(b,r)* is the joint probability of the coincidence of both events. $I(B_i; R)$ quantifies the reduction of uncertainty about the behavioural/neural response that can be gained from knowledge of the visibility of

pixel *i*.

Here, we calculated several MI quantities in single participants: MI(PIX, RT) to establish the relationship between image pixels and reaction times; MI(PIX, CORRECT) to establish the relationship between image pixels and correct responses; MI(PIX, RESP) between pixels and response category; and MI(PIX, ERP) to establish the relationship between image pixels and ERPs. These quantities were computed separately for face and noise trials. To control for the variable number of trials in each participant arising as a result of EEG preprocessing, we scaled every MI quantity for every participant by a factor of *2Nln2* (Ince, Mazzoni, Bartels, Logothetis, & Panzeri, 2012), using the formula:

$$MI_{scaled} = MI \times 2 \times Nt \times \log_2,$$

where *MI* refers to mutual information values, and *Nt* is the number of trials. MI_{scaled}, therefore, reflects a measure of MI adjusted for a systematic upward bias in the information estimate that might arise due to limited data sampling, especially if the numbers of trials in the two age groups are systematically different. It also converts MI to be the effect size for a log-likelihood test of independence (Sokal & Rohlf, 2012). All group-difference analyses were performed using the scaled MI values.

Mutual Information: Classification images

We refer to MI between pixels and behaviour or ERPs as classification images: they reveal the image pixels associated with modulations of the responses. Classification images for the MI(PIX, ERP) analysis were computed at every time point within the first 400 ms following stimulus onset, using the non-causal and causal-filtered datasets, and at each of the 6 electrodes specified above. To provide a summary of the image pixels associated with the ERP distributions for every participant at every electrode, we saved the maximum MI across time points in the non-causal filtered dataset.

Single-subject analyses. In order to establish which parts of the classification image showed significant association with the behavioural performance or ERPs in face and noise trials, we performed a permutation test coupled with the Threshold-Free Cluster Enhancement (TFCE) technique (S. M. Smith & Nichols, 2009) on individual participants' data. First, the MI values were computed between the bubble masks and the response labels. The resulting classification images were then transformed with the TFCE technique. This technique boosts the height of spatially extended regions in the image without changing the location of their

maxima. As such, clustered pixels will get higher TFCE scores than individual ones, which combined with standard permutation testing alleviates the problem of multiple comparisons across many pixels (Pernet, Latinus, Nichols, & Rousselet, 2015; Rousselet et al., 2014; S. M. Smith & Nichols, 2009). TFCE parameters were E=1 and H=2. To estimate TFCE scores expected by chance, the trial labels were shuffled while keeping the bubble masks constant (permutation test). The MI values were then computed and TFCE-scored again. This procedure was performed 1000 times. On every iteration of the permutation test, we saved the maximum TFCE value across pixels in order to create a distribution of TFCE values under the null hypothesis that the variables (pixel MI values and behavioural or ERP responses) are statistically independent. To obtain the image pixels associated with the response at the arbitrary significance level of 0.05, the original TFCE scores were then compared against the 95th percentile of the permutation distribution.

Group analyses. To assess classification image differences between the two age groups, we first computed Cliff's *delta* on the MI values at every pixel separately. Similarly to the single-subject analyses, we then applied a permutation test to estimate differences in MI values expected by chance. To that end, we shuffled young and older participants' labels while keeping the classification images constant. Then, we computed Cliff's *delta* on permuted classification images and saved the maximum *delta* score. This procedure was performed 1000 times in order to obtain a distribution of maximum *delta* scores under the null hypothesis that there are no differences in the classification images of the two age groups. We then compared the original *delta* scores against the 95th percentile of the permutation distribution.

Reverse analysis

To quantify how the presence of the eyes modulated behavioural and brain responses, we ran a reverse analysis (Smith et al., 2004; Rousselet et al., 2014). First, we created the eye mask by centring a circle (radius = 15 pixels) on the pixel that showed the maximum MI value in the group-averaged MI(PIX, ERP) classification image, separately for the left and for the right eye. We then summed pixel values revealed through single-trial Bubble masks that fell within the boundaries of each eye mask independently, and within both eye masks together, to provide an estimate of eye region visibility. We then split these values into ten equally populated bins ranging from the lowest to the highest sum values and compute the median RT and the mean percent correct for each bin. Next, we quantified the effect of eye

visibility on behavioural judgments by calculating the RT and percent correct difference between the 10th and the 1st bin. We then repeated this analysis with single-trial ERP distributions: we averaged the ERPs corresponding to each bin, separately for the left and right lateral electrodes. We then computed the N170 amplitude and latency in every participant and for each eye mask, for the lowest (1st bin) and the highest (10th bin) sum values, separately for the left and right electrodes. Given that the N170 on Bubble trials was delayed with respect to that on practice trials in both groups, we defined the N170 as the minimum in the time window 150 to 250 ms following stimulus onset in ERPs low-pass filtered at 20 Hz using a fourth order Butterworth non-causal filter. We then computed the differences between high and low amplitude and latency values for each group separately.

ERP ONSET ANALYSES

We quantified ERP onsets using the causal-filtered datasets. To control for multiple comparisons, we used a bootstrap temporal clustering technique as implemented in LIMO EEG (Pernet et al., 2015; Pernet et al., 2011).

ERP_{STD} onset. To determine whether age-related differences in timing of MI accumulation reflect differences in the onset of afferent activity to the visual cortex or information accumulation at later stages of visual processing, we looked at the time course of the standard deviation across electrodes of the mean ERP (ERP_{STD}). ERP_{STD} provides a compact description of the global ERP response, summarizing each participant's evoked brain activity across electrodes in one vector. This analysis was based on the notion that early visual activity can be characterized by a sudden increase in standard deviation of the mean ERP across electrodes (Foxe & Simpson, 2002). We computed the ERP_{STD} time course for each individual participant and mean baseline centred it. Then, we localised the first peak whose minimum height was five times the height of any peak in the baseline. Then, using ARESLab toolbox (Jekabsons, 2015), we built a piecewise-linear regression model with three basis functions using the Multivariate Adaptive Regression Splines (MARS) (Friedman, 1991) method. Onsets were defined as the location in time of the first knot.

MI onset. We quantified MI onsets using the same technique as with ERP_{STD} onsets.

TOPOGRAPHIC ANALYSES

Topographic maps for each participant were computed from the whole-scalp MI(PIX, ERP) results at the individual MI peak latency. Individual topographic maps were normalised

between 0 and 1, interpolated and rendered in a 67 x 67 pixel image using the EEGLAB function *topoplot*, and then averaged across participants in each age group. Using the interpolated head maps, we then computed a hemispheric lateralisation index for each participant. First, we saved the maximum pixel intensity in the left and the right hemisphere (lower left and right quadrants of the interpolated image), excluding the midline. Then, we computed the lateralisation index in each group as the ratio $(MI_{left} - MI_{right}) / (MI_{left} + MI_{right})$.

ACKNOWLEDGMENTS

This work has been funded by the UK Biotechnology and Biological Sciences Research Council (BBSRC) grant BB/J018929/1 awarded to NJVR, GAR, and PGS. KJ was supported by the BBSRC Doctoral Training Partnership (WestBio) Studentship. PGS received support from the Wellcome Trust (Senior Investigator Award, UK; 107802) and the Multidisciplinary University Research Initiative/Engineering and Physical Sciences Research Council (USA, UK; 172046-01).

DATA SHARING

A reproducibility package with data and code will be available online as soon as possible.

REFERENCES

Acunzo, D. J., MacKenzie, G., & van Rossum, M. C. W. (2012). Systematic biases in early ERP and ERF components as a result of high-pass filtering. *Journal of Neuroscience Methods*, *209*(1), 212–218. http://doi.org/10.1016/j.jneumeth.2012.06.011

Bennett, P. J., Sekuler, R., & Sekuler, A. B. (2007). The effects of aging on motion detection and direction identification. *Vision Research*, *47*(6), 799–809. http://doi.org/10.1016/j.visres.2007.01.001

Bentin, S., Allison, T., Puce, A., Perez, E., & McCarthy, G. (1996). Electrophysiological studies of face perception in humans. *Journal of Cognitive Neuroscience*, *8*(6), 551–565.

Bieniek, M. M., Bennett, P. J., Sekuler, A. B., & Rousselet, G. A. (2015). A robust and representative lower bound on object processing speed in humans. *European Journal of Neuroscience*, 1–11. http://doi.org/10.1111/ejn.13100

Bieniek, M. M., Frei, L. S., & Rousselet, G. A. (2013). Early ERPs to faces: Aging, luminance, and individual differences. *Frontiers in Psychology*, *4*(MAY). http://doi.org/10.3389/fpsyg.2013.00268

Boutet, I., Taler, V., & Collin, C.A. (2015). On the particular vulnerability of face recognition in aging: a review of three hypotheses. *Frontiers in Psychology*, 6, 1139.

Brainard, D. H. (1997). The Psychophysics Toolbox. *Spatial Vision*, *10*(4), 433–436.

Burianová, H., Lee, Y., Grady, C. L., & Moscovitch, M. (2013). Age-related dedifferentiation and compensatory changes in the functional network underlying face processing. *Neurobiology of Aging*, *34*(12), 2759–2767. http://doi.org/10.1016/j.neurobiolaging.2013.06.016

Cabeza, R. (2002). Hemispheric asymmetry reduction in older adults: the HAROLD model. *Psychology and Aging*, *17*(1), 85–100. http://doi.org/10.1037/0882-7974.17.1.85

Chaby, L., Narme, P., & George, N. (2011). Older adults' configural processing of faces: role of second-order information. *Psychology and Aging*, *26*(1), 71–79. http://doi.org/10.1037/a0020873

Cliff, N. (1996). *Ordinal methods for behavioural data analysis*. Mahwah, NJ: Lawrence Erlbaum Associates.

Cover, T. M., & Thomas, J. A. (2006). *Elements of information theory* (2nd Edition). Wiley-Interscience.

Cremer, R., & Zeef, E. J. (1987). What Kind of Noise Increases With Age? *Journal of Gerontology*, *42*(5), 515–518.

Danziger, W. L., & Salthouse, T. A. (1978). Age and the perception of incomplete figures. *Exp Aging Res*, *4*(1), 67–80. http://doi.org/10.1080/03610737808257127

Davis, S. W., Dennis, N. A., Daselaar, S. M., Fleck, M. S., & Cabeza, R. (2008). Que PASA? The posterior-anterior shift in aging. *Cerebral Cortex* , *18*(5), 1201–9. http://doi.org/10.1093/cercor/bhm155

De Sanctis, P., Katz, R., Wylie, G. R., Sehatpour, P., Alexopoulos, G. S., & Foxe, J. J. (2008). Enhanced and bilateralized visual sensory processing in the ventral stream may be a feature of normal aging. *Neurobiology of Aging*, *29*(10), 1576–1586. http://doi.org/10.1016/j.neurobiolaging.2007.03.021

Delorme, A., & Makeig, S. (2004). EEGLAB: an open source toolbox for analysis of single-trial EEG dynamics including independent component analysis. *Journal of Neuroscience Methods*, *134*, 9–21. http://doi.org/10.1016/j.jneumeth.2003.10.009

Delorme, A., Mullen, T., Kothe, C., Akalin Acar, Z., Bigdely-Shamlo, N., Vankov, A., … Makeig, S. (2011). EEGLAB, SIFT, NFT, BCILAB, and ERICA: new tools for advanced EEG processing. *Computational Intelligence and Neuroscience*, *2011*, 130714. http://doi.org/10.1155/2011/130714

Delorme, A., Sejnowski, T., & Makeig, S. (2007). Enhanced detection of artifacts in EEG data using higher-order statistics and independent component analysis. *NeuroImage*, *34*(4), 1443–9. http://doi.org/10.1016/j.neuroimage.2006.11.004

Elliott, D. B., Sanderson, K., & Conkey, A. (1990). The reliability of the Pelli-Robson contrast sensitivity chart. *Ophthalmic and Physiological Optics*, *10*(1), 21–24. http://doi.org/10.1111/j.1475-1313.1990.tb01100.x

Foxe, J. J., & Simpson, G. V. (2002). Flow of activation from V1 to frontal cortex in humans:

A framework for defining “early” visual processing. *Experimental Brain Research*, *142*(1), 139–150. http://doi.org/10.1007/s00221-001-0906-7

Friedman, J. H. (1991). Multivariate Adaptive Regression Splines. *The Annals of Statistics*, *19*(1), 1–67. http://doi.org/10.1214/aos/1176347963

Garrett, D.D., Kovacevic, N., McIntosh, A.R., & Grady, C.L. (2010). Blood oxygen level-dependent signal variability is more than just noise. *Journal of Neuroscience*, 30(14), 4914-21.

Garrett D.D., Kovacevic N., McIntosh A.R., Grady C.L. (2013). The modulation of BOLD variability between cognitive states varies by age and processing speed. *Cerebral Cortex*, 23(3), 684–693.

Garrett, D.D., Lindenberger, U., Hoge, R.D., & Gauthier, C.J. (2017). Age differences in brain signal variability are robust to multiple vascular controls. *Scientific Reports*, 7: 10149.

Gazzaley, A., Clapp, W., Kelley, J., McEvoy, K., Knight, R. T., & D’Esposito, M. (2008). Age-related top-down suppression deficit in the early stages of cortical visual memory processing. *Proceedings of the National Academy of Sciences*, *105*(35), 13122–13126. http://doi.org/10.1073/pnas.0806074105

Gold, J., Bennett, P. J., & Sekuler, A. B. (1999). Identification of band-pass filtered letters and faces by human and ideal observers. *Vision Research*, *39*(21), 3537–3560. http://doi.org/10.1016/S0042-6989(99)00080-2

Gosselin, F., & Schyns, P. G. (2001). Bubbles: A technique to reveal the use of information in recognition tasks. *Vision Research*, *41*(17), 2261–2271. http://doi.org/10.1016/S0042-6989(01)00097-9

Grady, C. L., Randy McIntosh, A., Horwitz, B., & Rapoport, S. I. (2000). Age-Related Changes in the Neural Correlates of Degraded and Nondegraded Face Processing. *Cognitive Neuropsychology*, *17*(1–3), 165–186. http://doi.org/10.1080/026432900380553

Grady, C.L., & Garrett, D.D. (2014). Understanding variability in the BOLD signal and why it matters for aging. *Brain Imaging and Behavior*, 8(2), 274-83.

Groppe, D. M., Makeig, S., & Kutas, M. (2009). Identifying reliable independent components via split-half comparisons. *NeuroImage*, *45*(4), 1199–211. http://doi.org/10.1016/j.neuroimage.2008.12.038

Habak, C., Wilkinson, F., & Wilson, H. R. (2008). Aging disrupts the neural transformations that link facial identity across views. *Vision Research*, *48*(1), 9–15. http://doi.org/10.1016/j.visres.2007.10.007

Harrell, F. E., & Davis, C. E. (1982). A new distribution-free quantile estimator. *Biometrika*, *69*(3), 635–640. http://doi.org/10.1093/biomet/69.3.635

Huang, Y.-Z., Rothwell, J. C., Chen, R.-S., Lu, C.-S., & Chuang, W.-L. (2011). The theoretical model of theta burst form of repetitive transcranial magnetic stimulation. *Clinical Neurophysiology*, *122*(5), 1011–8. http://doi.org/10.1016/j.clinph.2010.08.016

Ince, R. A. A., Giordano, B. L., Kayser, C., Rousselet, G. A., Gross, J., & Schyns, P. G. (2017). A statistical framework for neuroimaging data analysis based on mutual information estimated via a gaussian copula. *Human Brain Mapping*, *38*(3), 1541–1573. http://doi.org/10.1002/hbm.23471

Ince, R. A. A., Jaworska, K., Gross, J., Panzeri, S., van Rijsbergen, N. J., Rousselet, G. A., & Schyns, P. G. (2016). The Deceptively Simple N170 Reflects Network Information Processing Mechanisms Involving Visual Feature Coding and Transfer Across Hemispheres. *Cerebral Cortex*. http://doi.org/10.1093/cercor/bhw196

Ince, R. A. A., Mazzoni, A., Bartels, A., Logothetis, N. K., & Panzeri, S. (2012). A novel test to determine the significance of neural selectivity to single and multiple potentially correlated stimulus features. *Journal of Neuroscience Methods*, *210*(1), 49–65. http://doi.org/10.1016/j.jneumeth.2011.11.013

Ince, R. A. A., Petersen, R. S., Swan, D. C., & Panzeri, S. (2009). Python for information theoretic analysis of neural data. *Frontiers in Neuroinformatics*, *3*, 4. http://doi.org/10.3389/neuro.11.004.2009

Itier, R. J., Alain, C., Sedore, K., & McIntosh, A. R. (2007). Early face processing specificity: It's in the eyes! *Journal of Cognitive Neuroscience*, *19*(11), 1815–1826. http://doi.org/10.1162/jocn.2007.19.11.1815

Jekabsons, G. (2015). ARESLab: Adaptive Regression Splines toolbox for Matlab/Octave.

Kayser, J. (2009). Current source density (CSD) interpolation using spherical splines - CSD Toolbox (Version 1.1). New York State Psychiatric Institute: Division of Cognitive Neuroscience.

Kayser, S. J., Ince, R. A. A., Gross, J., & Kayser, C. (2015). Irregular Speech Rate Dissociates Auditory Cortical Entrainment, Evoked Responses, and Frontal Alpha. *Journal of Neuroscience*, *35*(44). Retrieved from http://www.jneurosci.org/content/35/44/14691

Kleiner, M., Brainard, D. H., & Pelli, D. (2007). What's new in Psychtoolbox-3? *Perception*, *36*(ECVP Abstract Supplement).

Kolev, V., Falkenstein, M., & Yordanova, J. (2006). Motor-response generation as a source of aging-related behavioural slowing in choice-reaction tasks. *Neurobiology of Aging*, *27*(11), 1719–1730. http://doi.org/10.1016/j.neurobiolaging.2005.09.027

Koretz, J.F., Kaufman, P.L., Neider, M.W., & Goeckner, P.A. (1989). Accommodation and presbyopia in the human eye – aging of the anterior segment. *Vision Research*, 29(12), 1685-92.

Kurylo, D. D. (2006). Effects of aging on perceptual organization: efficacy of stimulus features. *Experimental Aging Research*, *32*(2), 137–52. http://doi.org/10.1080/03610730600553901

Li, S. C., Lindenberger, U., & Sikström, S. (2001). Aging cognition: from neuromodulation to representation. *Trends in Cognitive Sciences*, *5*(11), 479–486. Retrieved from http://www.ncbi.nlm.nih.gov/pubmed/11684480

Lindfield, K. C., & Wingfield, A. (1999). An experimental and computational analysis of age differences in the recognition of fragmented pictures: inhibitory connections versus speed of processing. *Experimental Aging Research*, *25*(3), 223–42. http://doi.org/10.1080/036107399244002

Lindfield, K. C., Wingfield, A., & Bowles, N. L. (1994). Identification of fragmented pictures under ascending versus fixed presentation in young and elderly adults: Evidence for the inhibition-deficit hypothesis. *Aging, Neuropsychology, and Cognition*, *1*(4), 282–291. http://doi.org/10.1080/13825589408256582

Lott, L. A., Haegerstrom-Portnoy, G., Schneck, M. E., & Brabyn, J. A. (2005). Face

recognition in the elderly. *Optometry and Vision Science*, *82*(10), 874–881.

Luck, S. J. (2005). *An introduction to the event-related potential technique*. MIT Press.

Lustig, C., Hasher, L., & Zacks, R. T. (2007). Inhibitory deficit theory: Recent developments in a “new view.” *Inhibition in Cognition*, (571), 145–162. http://doi.org/http://dx.doi.org/10.1037/11587-008

Morcom, A.M., Cambridge Centre for Ageing and Neuroscience (Cam-CAN), & Henson, R.N. (2017). Increased prefrontal activity with aging reflects nonspecific neural responses rather than compensation. bioRxiv 156935, doi: https://doi.org/10.1101/156935

Nakamura, A., Yamada, T., Abe, Y., Nakamura, K., Sato, N., Horibe, K., … Ito, K. (2001). Age-related changes in brain neuromagnetic responses to face perception in humans. *Neuroscience Letters* (Vol. 312). http://doi.org/10.1016/S0304-3940(01)02168-1

Norton, D., McBain, R., & Chen, Y. (2009). Reduced ability to detect facial configuration in middle-aged and elderly individuals: Associations with spatiotemporal visual processing. *The Journals of Gerontology Series B: Psychological Sciences and Social Sciences*, 64B(3), 328-334.

Obermeyer, S., Kolling, T., Schaich, A., & Knopf, M. (2012). Differences between old and young adults’ ability to recognize human faces underlie processing of horizontal information. *Frontiers in Aging Neuroscience*, *4*(APR), 1–9. http://doi.org/10.3389/fnagi.2012.00003

Owsley, C., Sekuler, R., & Boldt, C. (1981). Aging and low-contrast vision: face perception. *Investigative Ophthalmology and Visual Science*, *21*(2), 362–365.

Pakkenberg, B., & Gundersen, H. J. G. (1997). Neocortical neuron number in humans: Effect of sex and age. *The Journal of Comparative Neurology*, *384*(2), 312–320. http://doi.org/10.1002/(SICI)1096-9861(19970728)384:2<312::AID-CNE10>3.0.CO;2-K

Park, D. C., Polk, T. A., Park, R., Minear, M., Savage, A., & Smith, M. R. (2004). Aging reduces neural specialization in ventral visual cortex. *Proceedings of the National Academy of Sciences of the United States of America*, *101*(35), 13091–5. http://doi.org/10.1073/pnas.0405148101

Park, H., Ince, R. A. A., Schyns, P. G., Thut, G., & Gross, J. (2015). Frontal Top-Down Signals Increase Coupling of Auditory Low-Frequency Oscillations to Continuous Speech in Human Listeners. *Current Biology* (Vol. 25). http://doi.org/10.1016/j.cub.2015.04.049

Park, J., Carp, J., Kennedy, K. M., Rodrigue, K. M., Bischof, G. N., Huang, C.-M., … Park, D. C. (2012). Neural broadening or neural attenuation? Investigating age-related dedifferentiation in the face network in a large lifespan sample. *Journal of Neuroscience*, *32*(6), 2154–2158. http://doi.org/10.1523/JNEUROSCI.4494-11.2012

Pelli, D. G. (1997). The VideoToolbox software for visual psychophysics: transforming numbers into movies. *Spatial Vision*, *10*(4), 437–42. Retrieved from http://www.ncbi.nlm.nih.gov/pubmed/9176953

Pernet, C. R., Chauveau, N., Gaspar, C., Rousselet, G. A., Pernet, C. R., Chauveau, N., … Rousselet, G. A. (2011). LIMO EEG: a toolbox for hierarchical LInear MOdeling of ElectroEncephaloGraphic data. *Computational Intelligence and Neuroscience*, *2011*, 831409. http://doi.org/10.1155/2011/831409

Pernet, C. R., Latinus, M., Nichols, T. E., & Rousselet, G. A. (2015). Cluster-based computational methods for mass univariate analyses of event-related brain potentials/fields: A simulation study. *Journal of Neuroscience Methods*, *250*, 85–93. http://doi.org/10.1016/j.jneumeth.2014.08.003

Polat, U., Schor, C., Tong, J.L., Zomet, A., Lev, M., Yehezkel, O., Sterkin, A., & Levi, D.M. (2012). Training the brain to overcome the effect of aging on the human eye. *Scientific Reports*, 2: 278.

Roudaia, E., Bennett, P. J., & Sekuler, A. B. (2008). The effect of aging on contour integration. *Vision Research*, *48*(28), 2767–2774. http://doi.org/10.1016/j.visres.2008.07.026

Rousselet, G. A. (2012). Does Filtering Preclude Us from Studying ERP Time-Courses? *Frontiers in Psychology*, *3*, 131. http://doi.org/10.3389/fpsyg.2012.00131

Rousselet, G. A., Gaspar, C. M., Pernet, C. R., Husk, J. S., Bennett, P. J., & Sekuler, A. B. (2010). Healthy aging delays scalp EEG sensitivity to noise in a face discrimination task. *Frontiers in Psychology*, *1*(JUL), 1–14. http://doi.org/10.3389/fpsyg.2010.00019

Rousselet, G. A., Husk, J. S., Pernet, C. R., Gaspar, C. M., Bennett, P. J., & Sekuler, A. B. (2009). Age-related delay in information accrual for faces: evidence from a parametric, single-trial EEG approach. *BMC Neuroscience*, *10*, 114. http://doi.org/10.1186/1471-2202-10-114

Rousselet, G. A., Ince, R. A. A., van Rijsbergen, N. J., & Schyns, P. G. (2014). Eye coding mechanisms in early human face event-related potentials. *Journal of Vision*, *14*(13), 1–24. http://doi.org/10.1167/14.13.7

Rousselet, G. A., Pernet, C. R., Bennett, P. J., & Sekuler, A. B. (2008). Parametric study of EEG sensitivity to phase noise during face processing. *BMC Neuroscience*, *9*, 98. http://doi.org/10.1186/1471-2202-9-98

Ruffman, T., Henry, J.D., Livingstone, V., & Philips, L.H. (2008). Meta-analytic review of emotion recognition in aging: implications for neuropsychological models of aging. *Neuroscience and Biobehavioral Reviews*, 32(4), 863-81.

Salthouse, T. a. (1996). The processing-speed theory of adult age differences in cognition. *Psychological Review*, *103*(3), 403–428. http://doi.org/10.1037/0033-295X.103.3.403

Salthouse, T. A., & Lichty, W. (1985). Tests of the neural noise hypothesis of age-related cognitive change. *Journal of Gerontology*, *40*(4), 443–450. http://doi.org/10.1093/geronj/40.4.443

Salthouse, T. A., & Meinz, E. J. (1995). Aging, Inhibition, Working Memory, and Speed, *50*(6), 297–306.

Salthouse, T. A., & Prill, K. A. (1988). Effects of aging on perceptual closure. *The American Journal of Psychology*, *101*(2), 217–238.

Schmolesky, M. T., Wang, Y., Pu, M., & Leventhal, A. G. (2000). Degradation of stimulus selectivity of visual cortical cells in senescent rhesus monkeys. *Nature Neuroscience*, *3*(4), 384–390. http://doi.org/10.1038/73957

Schyns, P. G., Petro, L. S., & Smith, M. L. (2007). Dynamics of Visual Information Integration in the Brain for Categorizing Facial Expressions. *Current Biology*, *17*(18), 1580–1585. http://doi.org/10.1016/j.cub.2007.08.048

Schyns, P. G., Thut, G., & Gross, J. (2011). Cracking the code of oscillatory activity. *PLoS*

Biology, *9*(5). http://doi.org/10.1371/journal.pbio.1001064

Sekuler, A. B., Gold, J. M., Murray, R. F., & Bennett, P. . (2000). Visual completion of partly occluded objects: insights from behavioral studies. *Neuro-Ophtalmology*, *23*, 165–168.

Sergent, J., Ohta, S., & MacDonald, B. (1992). Functional neuroanatomy of face and object processing. A positron emission tomography study. *Brain : A Journal of Neurology*, *115 Pt 1*(1), 15–36. http://doi.org/10.1093/brain/115.1.15

Slessor, G., Riby, D. M., & Finnerty, A. N. (2013). Age-related differences in processing face configuration: The importance of the eye region. *Journals of Gerontology - Series B Psychological Sciences and Social Sciences*, *68*(2), 228–231. http://doi.org/10.1093/geronb/gbs059

Smith, M. L., Gosselin, F., & Schyns, P. G. (2004). Receptive fields for flexible face categorizations. *Psychological Science*, *15*(11), 753–761. http://doi.org/10.1111/j.0956-7976.2004.00752.x

Smith, S. M., & Nichols, T. E. (2009). Threshold-free cluster enhancement: Addressing problems of smoothing, threshold dependence and localisation in cluster inference. *NeuroImage*, *44*(1), 83–98. http://doi.org/10.1016/j.neuroimage.2008.03.061

Sokal, R. R., & Rohlf, F. J. (2012). *Biometry : the principles and practice of statistics in biological research* (4th Edition). W.H. Freeman.

Takahashi, T., Cho, R.Y., Murata, T., Mizuno, T., Kukuchi, M., Mizukami, K., Kosaka, H., Takahashi, K., & Wada, Y. (2009). Age-related variation in EEG complexity to photic stimulation: A multiscale entropy analysis. *Clinical Neurophysiology*, 120(3), 476-483.

Tang, H., Buia, C., Madhavan, R., Crone, N. E., Madsen, J. R., Anderson, W. S., & Kreiman, G. (2014). Spatiotemporal Dynamics Underlying Object Completion in Human Ventral Visual Cortex. *Neuron*, *83*(3), 736–748. http://doi.org/10.1016/j.neuron.2014.06.017

Tenke, C. E., & Kayser, J. (2012). Generator localization by current source density (CSD): implications of volume conduction and field closure at intracranial and scalp resolutions. *Clinical Neurophysiology*, *123*(12), 2328–45. http://doi.org/10.1016/j.clinph.2012.06.005

Van Rijsbergen, N. J., & Schyns, P. G. (2009). Dynamics of trimming the content of face representations for categorization in the brain. *PLoS Computational Biology*, *5*(11).

http://doi.org/10.1371/journal.pcbi.1000561

Wang, Y., Zhou, Y., Ma, Y., & Leventhal, A. G. (2005). Degradation of signal timing in cortical areas V1 and V2 of senescent monkeys. *Cerebral Cortex* , *15*(4), 403–8. http://doi.org/10.1093/cercor/bhh143

Whitfield, K. E., & Elias, J. W. (1992). Age cohort differences in the ability to perform closure on degraded figures. *Experimental Aging Research*, *18*(2), 67–73. http://doi.org/10.1080/03610739208253913

Widmann, A., & Schröger, E. (2012). Filter effects and filter artifacts in the analysis of electrophysiological data. *Frontiers in Psychology*, *3*, 233. http://doi.org/10.3389/fpsyg.2012.00233

Wiese, H., Schweinberger, S. R., & Hansen, K. (2008). The age of the beholder: ERP evidence of an own-age bias in face memory. *Neuropsychologia*, *46*(12), 2973–2985. http://doi.org/10.1016/j.neuropsychologia.2008.06.007

Wilcox, R. R. (2006). Graphical Methods for Assessing Effect Size: Some Alternatives to Cohen's d. *Journal of Experimental Education*, *74*(4), 353–367. Retrieved from http://ezproxy.library.capella.edu/login?url=http://search.ebscohost.com/login.aspx?direct=true&db=aph&AN=21333704&site=ehost-live&scope=site

Wilcox, R. R. (2012). *Introduction to robust estimation and hypothesis testing*. Academic Press.

Wilson, H. R., Mei, M., Habak, C., & Wilkinson, F. (2011). Visual bandwidths for face orientation increase during healthy aging. *Vision Research*, *51*(1), 160–164. http://doi.org/10.1016/j.visres.2010.10.026

Yang, Y., Liang, Z., Li, G., Wang, Y., Zhou, Y., & Leventhal, A. G. (2008). Aging affects contrast response functions and adaptation of middle temporal visual area neurons in rhesus monkeys. *Neuroscience*, *156*(3), 748–757. http://doi.org/10.1016/j.neuroscience.2008.08.007